PARTICLE SIZE CHARACTERIZATION OF SUSPENSIONS USING ULTRASONIC METHOD

A THESIS SUBMITTED TO
THE GRADUATE SCHOOL OF NATURAL AND APPLIED SCIENCES
OF
MIDDLE EAST TECHNICAL UNIVERSITY

BY

ESMA ÖZÇELİK

IN PARTIAL FULFILLMENT OF THE REQUIREMENTS
FOR
THE DEGREE OF MASTER OF SCIENCE
IN
CHEMICAL ENGINEERING

DECEMBER 2019

Approval of the thesis:

PARTICLE SIZE CHARACTERIZATION OF SUSPENSIONS USING ULTRASONIC METHOD

submitted by **ESMA ÖZÇELİK** in partial fulfillment of the requirements for the degree of **Master of Science in Chemical Engineering Department, Middle East Technical University** by,

Prof. Dr. Halil Kalıpçılar
Dean, Graduate School of **Natural and Applied Sciences** _____

Prof. Dr. Pınar Çalık
Head of Department, **Chemical Engineering** _____

Prof. Dr. Yusuf Uludağ
Supervisor, **Chemical Engineering, METU** _____

Examining Committee Members:

Prof. Dr. Halil Kalıpçılar
Chemical Engineering, METU _____

Prof. Dr. Yusuf Uludağ
Chemical Engineering, METU _____

Assoc. Prof. Dr. Erhan Bat
Chemical Engineering, METU _____

Assoc. Prof. Dr. Berna Topuz
Chemical Engineering, Ankara University _____

Assist. Prof. Dr. İnci Ayrancı Tansık
Chemical Engineering, METU _____

Date: 06.12.2019

I hereby declare that all information in this document has been obtained and presented in accordance with academic rules and ethical conduct. I also declare that, as required by these rules and conduct, I have fully cited and referenced all material and results that are not original to this work.

Name, Surname: Esma Özçelik

Signature:

ABSTRACT

PARTICLE SIZE CHARACTERIZATION OF SUSPENSIONS USING ULTRASONIC METHOD

Özçelik, Esma
Master of Science, Chemical Engineering
Supervisor: Prof. Dr. Yusuf Uludağ

December 2019, 69 pages

Particle size is very important in many areas of industry and production processes in industries. For example, medicine, paint, etc. Therefore, it is important to obtain the particle size in a suspension. Particle size analysis can be performed by different methods. The aim of this study is to determine particle size by combining data from ultrasonic method and settling information. The fact that the ultrasonic method is cheap, non-destructive and non-invasive makes ultrasonic method very advantageous.

In this study, sand was chosen for particle size analysis. Firstly, density was calculated from the void ratio of sand. Sieve analysis was performed for sand particles and a mixture of sand with different particle size range of 38 μm to 150 μm and 38 μm to 90 μm were prepared.

The attenuation of the sound waves when the ultrasonic method enters an environment is based on the loss of energy. This method is used by taking measurements using Ultrasonic Instrument (UDV), DOP 2000 device. These measurements were performed by recording the intensity of ultrasound waves at 1 MHz at constant frequency. As the concentration increases, the attenuation rate of the sound wave increases. In order to use these measurements in sand suspension, 1%, 0.75%, 0.5%

0.25% 0.125% and 0.0625% weight percent suspensions were prepared and calibrated. After the calibration was completed, %1 weight percent sand suspension was prepared.

This suspension was placed in the test apparatus and fixed to this apparatus in the ultrasonic probe and measurements were taken from the first to the thirtieth minute. Inspired by the Andreasen pipette method, continuous ultrasonic measurements were carried out instead of taking samples continuously from the suspension. Particle size analysis was performed by combining Andreasen pipette method, settling data and ultrasonic method. The experiment was performed three times for repeatability.

According to sieve analysis, particle mixture contains 4.61% particle size between 38 μm to 63 μm, 27.56% particle size between 63 μm to 90 μm and 67.83% particle size between 90 μm to 150 μm The first settling experiment with 1% sand suspension, results reveal that, the 66% of the suspension contains particle sizes between 24.3 μm to 42 μm, 16.6% of the suspension contains the particles in the size of 42 μm to 59.5 μm and 8.8% of particles in the range of 59.5 μm to 150 μm.

For the second sieve analysis, that is in the range of 38 μm to 90 μm, mixture of sand particles was prepared. Majority of the mixture contains particle size between 90 μm and 75 μm. Another set of experiments with 2% sand suspension of the particle mixture in the range of 38 μm to 90 μm are performed and the results indicate that, the suspension contains 46.2% of particles in the range of 90 μm to 59.5 μm. 24.2% of the suspension contains the particles in the size of 59.5 μm to 42 μm. 16.6% of the suspension contains particle sizes between 42 μm to 37.6 μm. 12.9% of the suspension represents the particles smaller than the 37.6 μm. Settling experiments shows that generality of the suspension contains particle size between 90 μm to 59.5 μm that is 46.2% percent. On the other hand, according to sieve analysis there should be no particles smaller than the 38 μm however, from settling experiments 12.9% of particle mixture has a particle size smaller than 37.6 μm.

Keywords: Particle Size Distribution, Ultrasonic Measurements, Andreasen, Settling

ÖZ

SÜSPANSİYONLARDAKİ PARÇAÇIK DAĞILIMININ ULTRASONİK METOD İLE ARAŞTIRILMASI

Özçelik, Esma
Yüksek Lisans, Kimya Mühendisliği
Tez Danışmanı: Prof. Dr. Yusuf Uludağ

Aralık 2019, 69 sayfa

Parçacık büyüklüğü, endüstrinin birçok alanında ve endüstrilerdeki üretim süreçlerinde çok önemlidir. Örneğin ilaç, boya vb. Bu nedenle, bir süspansiyondaki parçacık boyutunun elde edilmesi önem arz etmektedir. Parçacık boyutu analizi değişik yöntemlerle gerçekleştirilebilir. Bu çalışmanın amacı, ultrasonik yöntem ve çökme bilgilerinden elde edilen verileri birleştirerek parçacık boyutunu tayin etmektir. Ultrasonik yöntemin ucuz, tahribatsız ve invazif olmaması ultrasonik yöntemi çok avantajlı kılmaktadır.

Bu çalışmada, parçacık boyutu analizi için kum seçilmiştir. Öncelikle, kumun boşluk oranından yoğunluk hesaplaması yapılmıştır. Kum parçacıkları için elek analizi yapılarak 38 μm ve 150 μm, 38 μm ve 90 μm bandında değişik parçacık boyutlarına sahip kum karışımları hazırlanmıştır.

Ultrasonik yöntem ses dalgalarının bir ortama girdiğinde zayıflaması, enerjisini yitirmesine dayanır. Bu metot Ultrasonik Cihaz (UDV), DOP 2000 cihazı kullanılarak ölçümler alınması ile kullanılmaktadır. Bu ölçümler sabit frekansta, 1 MHz'de ultra ses dalgalarının şiddetini kaydederek gerçekleştirilmiştir. Konsantrasyon arttıkça, ses dalgasındaki zayıflama oranının arttığı gözlenmiştir. Bu ölçümleri kum

süspansiyonunda kullanabilmek için, 1%, 0.75%, 0.5%, 0.25% 0.125% ve 0.0625% ağırlık yüzdeli süspansiyonlar hazırlanarak kalibrasyonu gerçekleştirilmiştir.

Kalibrasyon tamamlandıktan sonra, yüzde bir ağırlık yüzdeli kum süspansiyonu hazırlanmıştır. Bu süspansiyon, deney düzeneğine konulup, ultrasonik probunda bu düzeneğe sabitlenmesi sonucu ilk andan itibaren otuzuncu dakikaya kadar ölçümleri alınmıştır. Andreasen pipet yönteminden esinlenerek sürekli süspansiyondan örnek almak yerine sürekli ultrasonik ölçümleri gerçekleştirilmiştir. Buradaki hedef, kum süspansiyonunun çökmesinden ve ultrasonik ölçümlerin de alınarak iki yöntemin birbirine entegre edilmesi sonucu parçacık boyutu analizi yapmaktır. Andreasen pipet yöntemi, çökme verileri ve ultrasonik yöntem birleştirilerek parçacık boyutu analizi gerçekleştirilmiştir. Deney, tekrar edilebilirlik açısından üç kere yapılmıştır.

Elek analizine göre, partikül karışımı 38 μm den 63 μm arasında %4,61 oranında, partikül büyüklüğü 63 μm ile 90 μm arasında %27,56 oranında ve 90 μm ile 150 μm arasında %67,86 partikül büyüklüğü oranında içerdiği elde edilmiştir. %1 ağırlık yüzdeli kum süspansiyonu ile gerçekleştirlen çökme deneyi sonuçları ise; süspansiyonun % 66'sının 24.3 μm ile 42 μm arasında partikül boyutlarını içerdiğini, süspansiyonun % 16.6'sının 42 μm ile 59.5 μm boyutunda partikülleri içerdiğini ve 8,8% oranında 59.5 μm ile 150 μm aralığında partikül içerdiği sonucunu ortaya çıkarmıştır.

İkinci elek analizi için, 38 μm ila 90 μm aralığında, kum parçacıklarının karışımı hazırlandı. Karışımın büyük bir kısmı, 90 μm ile 75 μm arasında partikül büyüklüğü içermektedir. Parçacık karışımının 38 μm ila 90 μm aralığında %2 ağırlık yüzdeli kum süspansiyonu ile başka bir deney grubu gerçekleştirilmiştir ve sonuçlar, süspansiyonun %46.2 oranında 90 μm ila 59.5 μm aralığındaki parçacıkları içerdiğini göstermiştir. Süspansiyonun %24.2'si 59.5 μm ila 42 μm boyutunda parçacıklar içermektedir. Süspansiyonun %16.6'sı 42 μm ila 37.6 μm arasında parçacık büyüklüğü içermektedir. Süspansiyonun %12.9'u 37.6 μm'den daha küçük parçacıkları içerdiği ortaya çıkmıştır. Çökme deneyleri, süspansiyonun çoğunluğunun

90 μm ila 59.5 μm arasında bir partikül boyutu içerdiğini ve bunun %46.2 oranında olduğunu göstermektedir. Öte yandan, elek analizine göre 38 μm 'den daha küçük parçaçıkla olmamalıdır, ancak çökme deneylerinin %12.9'luk partikül karışımının 37.6 μm'den daha küçük parçaçık boyutuna sahip olduğunu göstermektedir.

Anahtar Kelimeler: Parçacık Büyüklüğü Dağılımı, Ultrasonik Ölçümler, Andreasen, Çöktürme

To my family…

ACKNOWLEDGEMENTS

Firstly, I would like to thank my supervisor Prof. Dr. Yusuf Uludağ for his patience, support, ideas and wonderful supervisions throughout my studies. During my studies, he always encouraged me to keep trying and to never give up therefore he is the best supervisor whom I could have had.

Secondly, I would like to thank my mother Nuriye Özçelik, my father Kemal Özçelik and my sister Ayşegül Öztürk for their never-ending support throughout my studies. Without their support and love I could not achieve this study.

TABLE OF CONTENTS

ABSTRACT v

ÖZ. viii

ACKNOWLEDGEMENTS xii

TABLE OF CONTENTS xiii

LIST OF TABLES xv

LIST OF FIGURES xvi

LIST OF ABBREVIATIONS xviii

LIST OF SYMBOLS xix

CHAPTERS

1. INTRODUCTION 1

2. SETTLING 5

2.1. Settling Phenomena in Particle Size Determination 5

2.2. Concentration changes with gravity settling and density gradient and concentration relation 9

2.3. Andreasen Pipette 11

2.4. Settling Velocity Determination 11

2.4.1. Settling Velocity Determination for Sand Particles used in the experiments 13

3. PSD DETERMINATION WITH ULTRASONIC METHODS 15

3.1. General Ultrasonic Theory 15

3.1.1. Sound 15

3.1.2. Ultrasound 16

3.1.3. Ultrasonic Wave Types 16
3.2. Attenuation 18
3.2.1. Absorption 19
3.2.2. Reflection 19
3.2.3. Scattering 21
3.3. Particle Size Determination with Attenuation Coefficient 22
4. EXPERIMENTAL METHODS 25
4.1. Void Fraction and Density Calculation of Sand 25
4.2. Void Fraction and Density Calculation of Sand 27
4.3. UDV DOP 2000 28
4.4. Experimental Procedure 29
4.4.1. Calibration of Sand Suspension 30
5. RESULTS AND DISCUSSION 35
6. CONCLUSIONS 55
REFERENCES 59
APPENDICES
A. Technical specifications DOP2000, model 2125 63
B. Error Margins for the Calibration Graphs 69

LIST OF TABLES

TABLES

Table 1: Settling velocities and Reynolds number for sand particles 13
Table 2: Sieve Analysis 1.....26
Table 3: Sieve Analysis 2.....27
Table 4: Void Fraction of sand particles 27
Table 5: Density Calculation of sand particles.....28
Table 6: Data of calibration suspensions 31
Table 7: Data of calibration suspensions of second set of experiments (2% sand suspension).....33
Table 8: Ultrasonic Instrument Set Values 35
Table 9: Different concentrated suspension Amplitude readings 36
Table 10: Calibration data with attenuation coefficient.....36
Table 11: Particle size range, concentration and percentage of each particle size range 44
Table 12: Weight Percent of particle size ranges from first sieve analysis.....45
Table 13: Particle size range, concentration and percentage of each particle size range 46
Table 14: Different concentrated suspension Amplitude readings 47
Table 15: Calibration data with attenuation coefficient.....47
Table 16: Particle size range, concentration and percentage of each particle size range 51
Table 17: Weight Percent of particle size ranges from second sieve analysis.....52

LIST OF FIGURES

FIGURES

Figure 1: Demonstration of Homogeneous, incremental gravitational sedimentation (Allen, 2003) 6
Figure 2: Andreasen Pipette 7
Figure 3: Demonstration of Homogeneous, incremental gravitational sedimentation (Allen, 2003) 8
Figure 4: Andreasen Pipette 9
Figure 5: Acoustic spectra representation (NDT Olympus, 2006) 15
Figure 6: Waves are illustrated in both distance or time (NDT Olympus, 2006) 16
Figure 7: Surface or Rayleigh Waves ("Modes of Sound Wave Propagation," n.d.) 17
Figure 8: Plate or Lamb waves ("Modes of Sound Wave Propagation," n.d.) 18
Figure 9: Illustration of transverse (shear) and longitudinal waves ("Wave Propagation," n.d.) 18
Figure 10: Reflection at two different acoustic impedances in two environments (Hwang, n.d.) 20
Figure 11: Reflection at two different acoustic impedances in two environments (Hwang, n.d.) 20
Figure 12: Single Scattering phenomena 21
Figure 13: Retsch Test Sieve 25
Figure 14: Retsch Sieve Shaker 26
Figure 15: UDV DOP 2000 28
Figure 16: Ultrasonic Probe 29
Figure 17: Plexiglass container 30
Figure 18: Experimental Setup 32
Figure 19: Calibration graph of sand suspensions at different concentration versus attenuation coefficient 37

Figure 20: Amplitude versus time of the settling of 1% weight percent sand suspension 38
Figure 21: Attenuation coefficient versus time of the settling experiment of 1% weight percent sand suspension 39
Figure 22: Concentration versus time of the settling experiment of 1% weight percent sand suspension.....39
Figure 23: Particle Size versus Time calculated according to Andreasen Equation.40
Figure 24: Attenuation coefficient comparison of three settling experiments.....41
Figure 25: Comparison of concentration values of three different settling experiments 42
Figure 26: Particle Size versus Concentration 43
Figure 27: Particle Size versus Particle Percentage 45
Figure 28: Amplitude versus time of the settling of 2% weight percent sand suspension for three different sets of experiments 48
Figure 29: Attenuation coefficient versus time of 2% sand suspension for three different set of experiments.....48
Figure 30: Calibration graph of sand suspensions at different concentration versus attenuation (for second set of experiments) 49
Figure 31: Concentration versus time of 2% sand suspension.....50
Figure 32: Particle Size versus Time calculated according to Andreasen Equation.51
Figure 33: Error Margins for the first calibration graph 69
Figure 34: Error Margins for the second calibration graph 69

LIST OF ABBREVIATIONS

ABBREVIATIONS

UDV	Ultrasonic Doppler Velocimetry
PRF	Pulse Repetition frequency
TGC	Time Gain Control
PSD	Particle Size Distribution

LIST OF SYMBOLS

SYMBOLS

A	Amplitude
C	Concentration of a suspension
f	Frequency
t	Time
h	Suspension height from ultrasonic probe to top
Re	Reynolds number
ρ	Fluid density
ρ_s	Particle density
g	Gravitational acceleration
W_s	Settling Velocity
m_s	Mass of solid to be dispersed
m_f	Mass of fluid to be dispersed
y	Concentration
x	Attenuation coefficient

GREEK LETTERS

ϕ	Density of a suspension
φ	Void Fraction
μ	Dynamic Viscosity

α Sound Attenuation

λ Wavelength

ρ Density

d Particle diameter

ν Kinematic viscosity of the fluid

SUBSCRIPTS

f Fluid

p Particle

w Water

CHAPTER 1

INTRODUCTION

Particle Size Distribution (PSD) of powdered solid materials is very important characteristic in performance of the products. For instance, particle size distribution has high importance for products such as cosmetics, pharmaceutical products, abrasives, ceramics, pigments, catalysts, and chemical reactants etc. (Testino, Alberto, Cervellino, & Ludwig, 2015). Therefore, particle size distribution of suspensions is very important in chemical industry.

Ultrasonic technology has been used in science and technology for a long time since the application areas of ultrasonic applications are increasing day by day. Ultrasonic waves can be named as the science of sound waves above the human limit of hearing (Duran et al., n.d.).

Currently, there are many diversities in measurement techniques of concentration and particle size distribution determination in suspensions or emulsions. On the other hand, most of them cannot provide information of particle size distribution or concentration data in high density suspensions (Weser, Wöckel, Hempel, Wessely, & Auge, 2013). Ultrasound techniques do not require dilution of suspensions. Dilution of suspension may lead to changes in sample construction or during dilution flocculation can occur. Therefore, ultrasonic methods can be used in highly concentrated suspensions without any dilution in order to determine particle size distribution (Povey, 2013).

Ultrasonic measurements of particle size distribution in a suspension has many benefits because this method is non-destructive and non-invasive. Also this method can be used to determine particle size distribution in opaque suspensions and suspensions with high concentrations (McClements, 1996).

Ultrasonic techniques offer a variety of desirable properties such as non-intrusive, rapid response to instant measurements, as well as the potential for measurement and control and application of radioactive reactors with high pressure and temperature conditions (Stolojanu & Prakash, 2001).

The ultrasound signal can penetrate through the walls of a container and indeed has the advantage of a non-invasive and non-destructive technique. An ultrasonic pulse of a given energy emitted from a source the transducer spreads into a medium through this medium and then reaches the receiver at low energy. The changes in the concentration of solids in a liquid change the density, which causes the media's compressibility as well as weakening of the speed and acoustic signal (Stolojanu & Prakash, 2001).

Ultrasonic methods that are used for particle size distribution of a suspension depends on attainment of the attenuation coefficient safely. Measurement of reduction in the amplitude of the ultrasonic wave travelling through a media leads to attenuation coefficient (McClements, 1996).

Settling of particles in a liquid or fluid, in other words suspension is used for particle size distribution determination. This phenomenon can be named as sedimentation and sedimentation can occur by an external force like gravity or centrifugal force on the particles. (Concha, 2009; CPS, 2007) Settling of particles in a fluid is used for particle size determination with Stokes' Law. In order to apply Stokes' Law, viscosity, density of the fluid is known, and time required for settling of particles in determined distance is measured. Gravitational sedimentation is restricted in manner of particle size. This restriction arises due to very small particle size which constitutes obstruction of effective settling due to large Brownian motion of very small particles. Also, very small particles settle so slow that the analysis time will take too long. Very small particles (<0.1 micron) cannot settle by gravity force, they will be suspended in the fluid and so they cannot be measured by gravitational sedimentation. Therefore, sedimentation method can be used for relatively larger particle sizes (CPS, 2007).

Accordingly, settling of particles, settling velocity of particles can be used for determination of particle size. Larger particles will settle firstly, then the smaller particles. In the thesis, particle size determination will be carried out with using the information from settling and the ultrasonic data from measurements of amplitudes from the UDV DOP 2000. Therefore, investigating the particle size distribution of suspensions by ultrasonic methods and settling phenomena is the objective of this study. Particle size is obtained by the settling time. With the help of the Ultrasonic Instrument, attenuation of different concentration values for the sand is obtained. Primarily, 1%, 0.75%, 0.5% 0.25% 0.125% and 0.0625% weight percent suspensions were prepared and each value representing the attenuation of the different concentrations are procured. This gives the calibration curve of different concentrations of sand suspensions. On the other hand, for 2% sand suspension different calibration with different weight percentages is carried out. In the experiments, at each time interval during 1% and 2% sand suspension settling, ultrasonic data is gained for different sets of experiments. Ultrasonic data of each time is given the attenuation coefficient and these attenuation coefficients are converged to concentration data by calibration curve for each time that the measurements are made. The theory used in Andreasen pipette method, that is taking samples of the suspension from an Andreasen pipette's bottom that is twenty centimeters, at predetermined time intervals, is converted to taking ultrasonic measurements of the suspension in the experimental setup at each time. Instead of taking samples from suspension during settling, ultrasonic instrument is used for obtaining amplitude data for each time. Amplitude data at each time interval is converted to attenuation to get concentration percentages of particle sizes. Therefore, emerging the time of settling to get particle size and the information of concentrations at different times during the settling is the method that is developed to achieve particle size distribution in this study.

CHAPTER 2

SETTLING

2.1. Settling Phenomena in Particle Size Determination

There are three forces acting on a particle when it is moving through a fluid that are drag force, gravity force and the buoyancy force (McCabe, Smith, & Harriott, n.d.). Particle size determination by the gravitational sedimentation methods are used with the dependence of settling properties of a single particle in a fluid under the effect of gravity. In the past so much experiments are carried out to find out the correlation between settling velocity and the particle. From these experiments unique relation has been revealed between Reynolds number and drag factor. That relation has generated the plain equation, the Stokes' Equation which can be applied at low Reynolds Number. Therefore, in the small Reynolds numbers region settling velocity of a single uniform spherical particle diameter is correspondent to its Stokes' diameter.

$$C_D = \frac{A}{Re} \tag{1}$$

$$d_t = \sqrt{\frac{18\mu h}{(\rho_p - \rho_f)gt}} \tag{2}$$

Fluid flow around the particle is not broken at the low Reynolds number and thus the flow is laminar. When the Reynolds number rises turbulence causes slower settling of the particle anticipated by the Stokes' Equation.

For this reason, homogeneous spherical particle's settling velocity is acknowledged then its particle size can be obtained. On the other hand, if the size is known settling velocity can be found.

The drag force on a particle relies on movement, thus non-spherical particles settles at a slow pace due to their largest cross-sectional area perpendicular to flow direction

than the particles settling with smallest area. From it is concluded that accumulation of same non-spherical particles, settling under laminar flow will have an interval of settling velocity depending on their movements.

There are several types of sedimentation techniques by gravity. In this thesis gravitational incremental sedimentation is investigated. This technique allows observation of the solids concentration at noted depth below surface of a preliminary homogeneous suspension by gravity settling.

Prior to arrival of the largest particle in the measurement area, the concentration of the suspension will stay same. At the time of particles settles from the measurement area, alike particles will enter the area, and this allows an equilibrium in the measurement area. Firstly, largest particles will settle due to having biggest mass within the all particles that results in decrease of concentration at time in the measurement area. Representation of a gravitational incremental sedimentation is given in the Figure 1 (Allen, 2003).

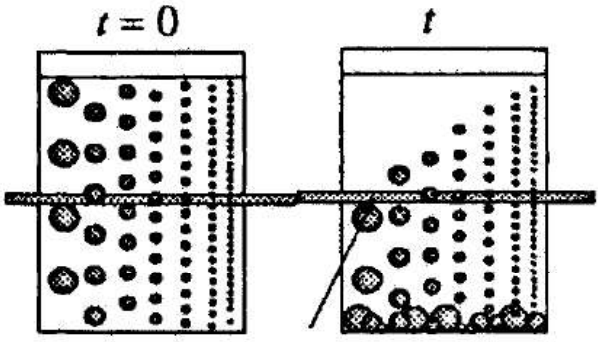

Figure 1: Demonstration of Homogeneous, incremental gravitational sedimentation (Allen, 2003)

For example, Andreasen Pipette technique can be given as the exemplification of homogeneous, incremental gravitational sedimentation. Also, Andreasen Pipette drawing is given in the Figure 2 (Allen, 2003).

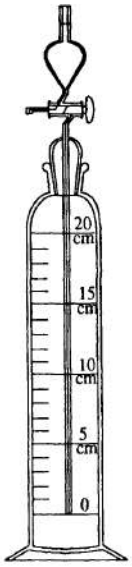

Figure 2: Andreasen Pipette

Particle size determination by the gravitational sedimentation methods are used with the dependence of settling properties of a single particle in a fluid under the effect of gravity. In the past so much experiments are carried out to find out the correlation between settling velocity and the particle. From these experiments unique relation has been revealed between Reynolds number and drag factor. That relation has generated the plain equation, the Stokes equation which can be applied at low Reynolds Number. Therefore, in the small Reynolds numbers region settling velocity of a single uniform spherical particle diameter is correspondent to its Stokes diameter.

Fluid flow around the particle is not broken at the low Reynolds number and thus the flow is laminar. When the Reynolds number rises turbulences causes the particle settling slower anticipated by the Stokes equation.

For this reason, homogeneous spherical particle's settling velocity is acknowledged then its particle size can be obtained. On the other hand, if the size is known settling velocity can be found.

The drag force on a particle relies on movement, thus non-spherical particles settles at a slow pace due to their largest cross-sectional area perpendicular to flow direction

than the particles settling with smallest area. From its concluded that accumulation of same non-spherical particles, settling under laminar flow will have an interval of settling velocity depending on their movements.

There are several types of sedimentation techniques by gravity. In this thesis gravitational incremental sedimentation is investigated. This technique allows to observation of the solids concentration at noted deepness below surface of a preliminary homogeneous suspension by gravity settling.

Prior to arrival of the largest particle in the measurement area, the concentration of the suspension will stay same. At the time of particles settles from the measurement area, alike particles will enter the area, and this allows an equilibrium in the measurement area. Firstly, largest particles will settle due to having biggest mass within the all particles that results in decrease of concentration at time in the measurement area. Representation of a gravitational incremental sedimentation is given at the figure below.(Allen, 2003)

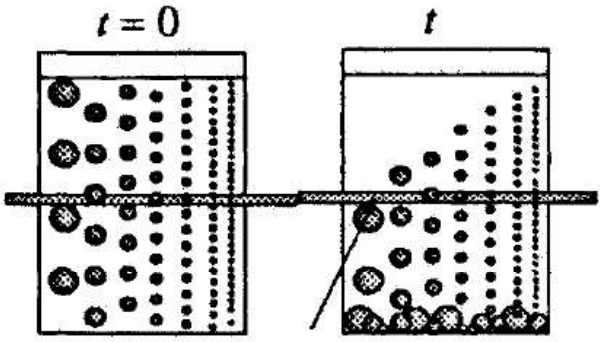

Figure 3: Demonstration of Homogeneous, incremental gravitational sedimentation (Allen, 2003)

For example, Andreasen Pipette technique can be given as the exemplification ı-of homogeneous, incremental gravitational sedimentation. Also, Andreasen Pipette drawing is given in the Figure 2. (Allen, 2003)

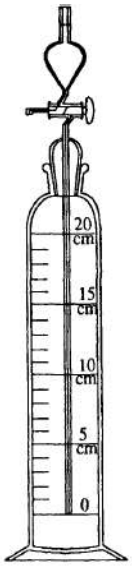

Figure 4: Andreasen Pipette

2.2. Concentration changes with gravity settling and density gradient and concentration relation

A suspension's concentration changes under gravity and relationship between concentration and density gradient in suspension is investigated below. (Allen, 2003)

$m_s = \rho_s v_s$ Mass of a powder to be dispersed (3)

$m_f = \rho_f v_f$ Mass of the fluid to be dispersed in (4)

At first mass concentration will be equal to;

$$d_{St}^2 = k(\frac{h}{t}) \quad (5)$$

At which concentration at deepness h, at time t equal to zero is $C(h, 0)$

A little horizontal element is studied at the deepness of h. In the beginning of sedimentation, particles settle from the element and they are stabled by the arrival of particles above. After the settling of largest particles settles from the horizontal element, there will be no particles to substitute them. Then concentration will decrease and will be equal to d_{St}.

d_{St} is defined as the size of the particle that settles at a velocity of h/t

In that case, suspension concentration at time t and deepness h can be written as;

$$C(h,t) = \frac{m_s'}{v_s'+v_f} = \int_{d_{min}}^{d_{St}} f(d)\mathrm{d}d \tag{6}$$

m_s' is defined as mass and v_s' is the volume of solids in a volume of fluid v_f at deeepness h from the top of suspension in the beginning of sedimentation.

$$C(h,0) = \frac{m_s}{v_s+v_f} = \int_{d_{min}}^{d_{max}} f(d)\mathrm{d}d \tag{7}$$

Equation 5& 7 leads to;

$$\frac{C(h,t)}{C(h,0)} = \frac{m_s'}{m_s} = \frac{\int_{d_{min}}^{d_{St}} f(d)\mathrm{d}d}{\int_{d_{min}}^{d_{max}} f(d)\mathrm{d}d} \tag{8}$$

Variation of v_s' and v_s is neglected according to the comparison of v_f . Hence, the graph of $C(h,t)/C(h,0)$ versus d_{St} leads to ratio of undersize Stokes' diameter by weight (Allen, 2003).

After Equation 6, density of the suspension can be defined as $\phi(h,t)$ at deepness h, at time t; (Allen, 2003).

$$\phi(h,t) = \frac{m_s'+m_f}{v_s'+v_f} \tag{9}$$

Mass of solids and the fluid are written as density times volumes then Equation 8 is obtained.

$$\phi(h,t) = \frac{\rho_s v_s'+\rho_f v_f}{v_s'+v_f} \tag{10}$$

$$\phi(h,t) = \frac{\rho_f(v_s'+v_f)+(\rho_s-\rho_f)v_s'}{v_s'+v_f} \tag{11}$$

$$\phi(h,t) = \rho_f + \frac{\rho_s-\rho_f}{\rho_s}\frac{m_s'}{v_s'+v_f} \tag{12}$$

$$\phi(h,t) = \rho_f + \frac{(\rho_s-\rho_f)}{\rho_s}C(h,t) \tag{13}$$

Density of the suspension can be defined as $\phi(h,t)$ at deepness h, at time t is obtained in the form of $C(h,t)$, also this derivation is executed for density of the suspension at deepness h and time zero.

$$\phi(h,0) = \frac{m_s+m_f}{v_s+v_f} \tag{14}$$

$$\phi(h,0) = \frac{\rho_s v_s+\rho_f v_f}{v_s+v_f} \tag{15}$$

$$\phi(h,0) = \frac{\rho_f(v_s+v_f)+(\rho_s-\rho_f)v_s}{v_s+v_f} \tag{16}$$

$$\phi(h,0) = \rho_f + \frac{\rho_s-\rho_f}{\rho_s}\,\frac{m_s}{v_s+v_f} \tag{17}$$

$$\phi(h,0) = \rho_f + \frac{(\rho_s-\rho_f)}{\rho_s}\,C(h,0) \tag{18}$$

Accordingly, combining Eq. 13 and 18

$$\frac{C(h,t)}{C(h,0)} = \phi = \frac{\phi(h,t)-\rho_f}{\phi(h,0)-\rho_f} \tag{19}$$

Density of the suspension (ϕ) is the mass fraction undersize d_{St} and defined by Equation 19.

2.3. Andreasen Pipette

Andreasen pipette, special size, half liter is a cylindrical glass container. Located at the top from the bottom of the suspension into a 10 ml container designed to extract samples. In the experiments, the suspension containing solids, at defined time intervals samples are taken out of the Andreasen pipette and the sample sizing is done with Stokes equation. Method has the same principle operation with decantation. But Andreasen pipette design, the experiments are more controlled and simple way. Compared to other methods, low cost is the biggest advantage of the Andreasen Pipette method. (Saklara, Bayraktara, & Öner, 2000) Also, Andreasen pipette uses the height of 20 centimeters of settling in the experiments.

2.4. Settling Velocity Determination

A single particle's settling velocity is identified as W_s . The particles drag coefficient is C_D. Reynolds Number (Re) is reversely proportional to drag coefficient. (Zhiyao, Tingting, Fumin, & Ruijie, 2015) Reynolds Number is defined by Equation 20.

$$Re = \frac{W_s d}{\nu} \tag{20}$$

Reynolds Number defines the flow properties around the particle. There are three types of flow properties that are laminar, transition and turbulent regime around the particle.

Drag coefficient is given in the equation below:

$$C_D = \frac{4}{3}\frac{\Delta \rho d g}{{W_s}^2} \tag{21}$$

Where $\Delta = \frac{\rho_s}{\rho} - 1$ (22)

There are two different equation defining C_D according to particle's Reynolds number.

- For Stokes flow ($Re < 1$);
  $C_D = \frac{A}{Re}$ (23)
- For Turbulent flow ($10^5 < Re < 2 * 10^5$);
  $C_D = B$ (24)

A and B are constants.

For Stokes flow conditions;

$${W_s}^2 = \frac{4}{3}\frac{\Delta \rho d g}{C_D} \; and \; C_D = \frac{A}{Re} \tag{25}$$

$${W_s}^2 = \frac{4}{3}\frac{\Delta \rho d \; Re}{A} \; and \; Re = \frac{W_s d}{\nu} \tag{26}$$

Settling velocity for Stokes flow;

$$W_s = \frac{4}{3A}\frac{\Delta \rho d^2}{\nu} \tag{27}$$

Settling velocity for turbulent flow;

$${W_s}^2 = \frac{4}{3}\frac{\Delta \rho d}{C_D} \; and \; C_D = B \tag{28}$$

$$W_s = \sqrt{\frac{4}{3}\frac{\Delta \rho d}{B}} \tag{29}$$

2.4.1. Settling Velocity Determination for Sand Particles used in the experiments

Generally, shape of factor of natural sand particles is less than unity and this leads that value of constant A is about 32 (Cheng, n.d.). For W_s calculation for sand particles A constant is taken as 32. Density of the sand particles is 2729 kg/m^3 and the calculation of settling velocities and Reynolds number for maximum particle sizes that are 150 μm and 90 μm; minimum particle size that is 38 μm of both sets of experiments are given in the table below. In these calculations water properties, such as density and viscosity, are evaluated at room temperature. Also, hindered settling for the particles is assumed to be negligible.

Table 1: Settling velocities and Reynolds number for sand particles

Particle Size (μm)	Settling Velocity, W_s (m/s)	Reynolds Number
150	0.0160	2.370
90	0.0057	0.511
38	0.0010	0.038

Reynolds number for 90 μm and 38 μm is smaller than 1 and the Stokes' Equation can be applied. For 150 μm particles Reynolds number is not smaller than 1. On the other hand, its value of 2.37 is still assumed to be sufficiently small to apply Stokes' Equation.

In sedimentation methods, sedimentation data with respect to time is taken at a known height h below the surface. Sedimentation methods that are used for particle size tests, settling of particles in the suspension creates concentration differences which leads to Stokes' diameter distribution of solids in the suspension. (Ulusoy, Yekeler, Biçer, & Gülsoy, 2007) This type of analysis is derived from the Stokes' Law that is given in the Equation 30 and the Equation 31.

$$d_t = \sqrt{\frac{18\mu h}{(\rho_p - \rho_f) g t}} \tag{30}$$

$$v = \frac{{d_t}^2 g\,(\rho_p - \rho_f)}{18\mu} = \frac{h}{t} \tag{31}$$

CHAPTER 3

PSD DETERMINATION WITH ULTRASONIC METHODS

3.1. General Ultrasonic Theory

3.1.1. Sound

Sound proceeds through an environment in the form of variation of pressure field. Environment of propagation can be water, tissue, air, human tissue or metal (Krishnamoorthy, Schmall, & Surti, 2016). As shown in Figure 3, classification of sound made according to different frequency values that are; infrasound (0-20 Hz), audible sound (20 – 20 kHz), ultrasound (greater than 20 kHz). People can only hear the sounds in the range of audible sound, they cannot hear either in the infrasonic region neither the ultrasonic region (Krishnamoorthy et al., 2016).

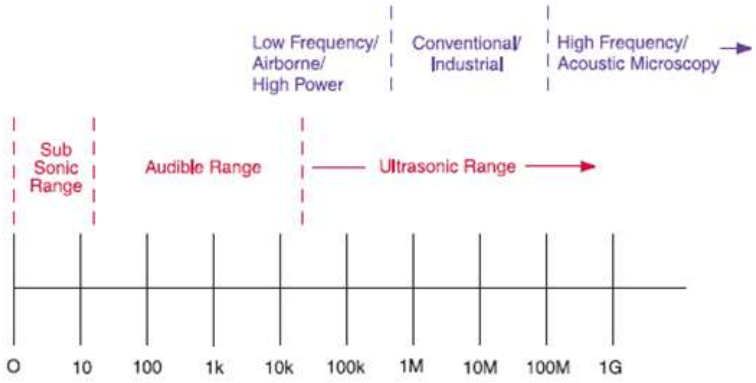

Figure 5: Acoustic spectra representation (NDT Olympus, 2006)

3.1.2. Ultrasound

The ultrasound is a kind of energy that its frequency is above the human hearing generated from the mechanical vibrations (Duran et al., n.d.).

Progression of ultrasound occurs from the dislocation and fluctuation of molecules from their normal position and then consecutive molecules dislocation and fluctuation in the direction of travelling path of ultrasound waves (Hwang, n.d.).

Characteristics of waves can be used to define ultrasound waves and it is illustrated in Figure 4 (NDT Olympus, 2006).

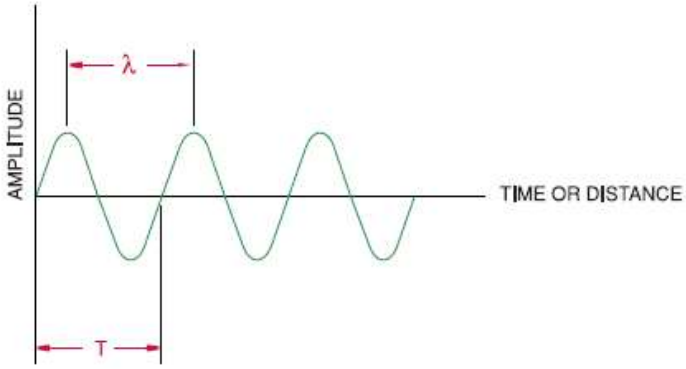

Figure 6: Waves are illustrated in both distance or time (NDT Olympus, 2006).

3.1.3. Ultrasonic Wave Types

Ultrasonic methods depend on vibration in the materials which is defined as acoustics. Sound waves progress through an environment in four main elements stated by the fluctuation of the particles. These four elements are transverse (shear) waves, longitudinal waves, surface waves and plate waves (Duran et al., n.d.).

- Longitudinal wave

The direction of vibration and propagation is the same. It is also called the pressure wave. Progression of this type wave can be in solid, liquid and gas. Everyday life

sound waves are longitudinal waves. The transmission rate is higher than other ultrasonic waves (Duran et al., n.d.).

- Transverse Wave

The direction of vibration and propagation are perpendicular to each other. This is also called a shear wave. Only in solid environments. It cannot be released in liquids and gases. The transmission rate is about half the longitudinal wave (Duran et al., n.d.).

- Surface (or Rayleigh) Wave

Vibration movement is an ellipse perpendicular to the direction of propagation. As the amplitude changes, the ellipse grows, becomes smaller, or becomes zero. This name is given only because they do not penetrate the material depth. Approximately one wavelength depth vibration of the material, i.e. ultrasonic energy is zero. Speed of this kind of waves is slightly smaller than transverse waves (Duran et al., n.d.).

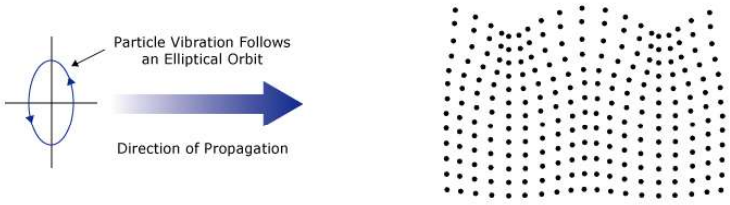

Figure 7: Surface or Rayleigh Waves ("Modes of Sound Wave Propagation," n.d.)

- Plate (or Lamb) Wave

Lamb waves are alike surface waves; however, they can be obtained only in thin plates (Hijazi, n.d.).

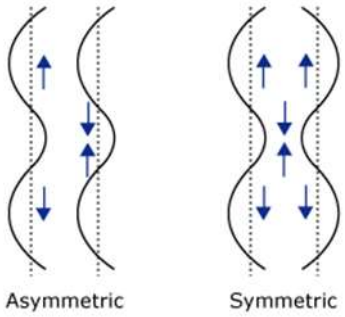

Figure 8: Plate or Lamb waves ("Modes of Sound Wave Propagation," n.d.)

In ultrasonic methods; transverse and longitudinal waves are commonly used. These waves are shown in the figure below ("Wave Propagation," n.d.).

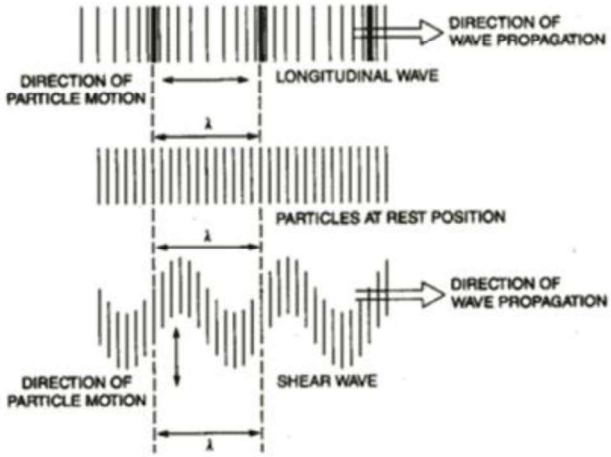

Figure 9: Illustration of transverse (shear) and longitudinal waves ("Wave Propagation," n.d.)

3.2. Attenuation

Energy loss arises as sound progresses through an environment and it is called attenuation (Powles, Martin, Wells, & Goodwin, 2018). When an ultrasound beam penetrates an environment, energy reduction is achieved by scattering, absorption and reflection. Any mechanism that causes reduction in ultrasonic is called as attenuation (Hendee & Ritenour, 2002).The ultrasound passing through the surface some of its energy is absorbed by the surface and the absorbed energy emerges as heat or particle

motion increase and it is called absorption (Duran et al., n.d.; Hendee & Ritenour, 2002).The second factor that leads to attenuation is scattering and the amount of energy passing through an environment will be reduced (Duran et al., n.d.).

The third factor that causes the attenuation is the reflection of the ultrasound beam in a systematic diversion (Duran et al., n.d.; Hendee & Ritenour, 2002).

3.2.1. Absorption

Absorption mechanism can be explained as when ultrasound wave passes through an environment, some of its energy is absorbed by the media which culminates in heat production (Hwang, n.d.; Taylor, 2012). Ultrasonic wave propagation results the particle in the media to move and it results the potential energy converted from kinetic energy. This Conversion occurs due to the compression of the molecules. When the highest compression occurrence, potential energy is at its maximum and also, kinetic energy is at its minimum. Molecules movement from their compressed place to their initial place is this time needs to kinetic energy converted from potential energy. Frequently, dissipation of energy from energy conversions are turned out as heat. This summarizes the absorption in ultrasound mechanisms (Kahn & Salgo, 2013).

3.2.2. Reflection

Part of sound energy reflected on interface between two different environments depends on the difference in acoustic impedance of these environments to the Acoustic impedance (Z) means that resilience product of its intensity and is the velocity of sound wave during propagating through an environment.(Hwang, n.d.; Powles et al., 2018)

$$Z = \rho c \tag{32}$$

Reflection mechanism occurs when ultrasound waves passing through two different environments which have different acoustic impedances (Hwang, n.d.). More energy will be reflected when two different environments have larger difference in acoustic impedances (Taylor, 2012).

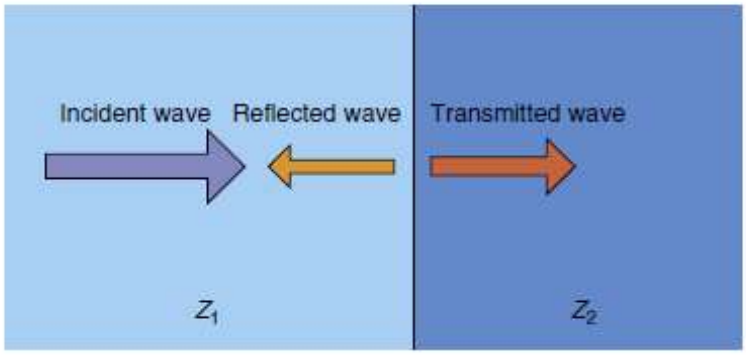

Figure 10: Reflection at two different acoustic impedances in two environments (Hwang, n.d.)

Reflection mechanism occurs when ultrasound waves passing through two different environments which have different acoustic impedances.(Hwang, n.d.) More energy will be reflected when two different environments have larger difference in acoustic impedances. (Taylor, 2012)

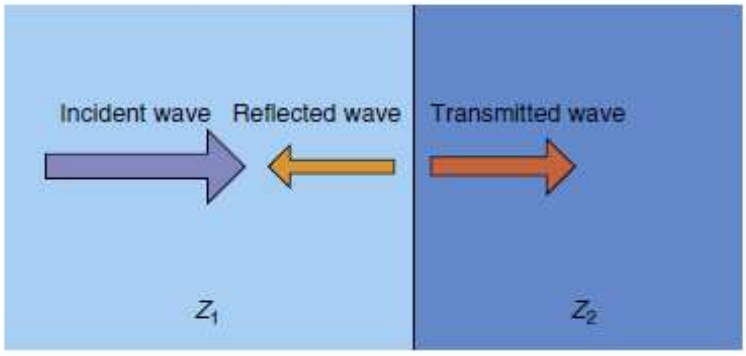

Figure 11: Reflection at two different acoustic impedances in two environments (Hwang, n.d.)

3.2.3. Scattering

Scattering, also referred to as reflection not echoing, is an emitted ultrasound wave that can interact with different elements in the media are smaller than the wavelength and have different impedance values from the medium to be propagated (Hwang, n.d.). Scatterer has a fluctuating behavior which is differing from the environment causes a wave to be named as scattering wave (Laugier & Haïat, 2011).

When an ultrasound wave interacts with a scatterer, a small portion of the acoustic density returns during contact of an ultrasound wave and the particle/scatterer, only a little part of the acoustic intensity returns or reflected to the transducer. Moreover, an ultrasonic wave that has scattered by a particle/scatterer, it happens to be scattering versatile ways generally (Hwang, n.d.). When an ultrasonic beam passes through an media, and the beam encounters with the particle/scatterer size difference between ultrasonic wavelength and the particle affects the scattering mechanism. Moreover, in multiple ways scattering occurs (Kahn & Salgo, 2013).

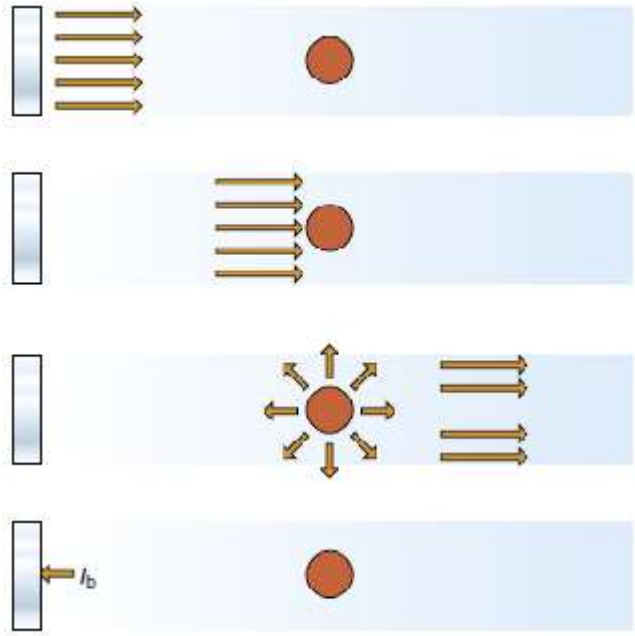

Figure 12: Single Scattering phenomena

In Figure 9, first the ultrasound beam exited from the transducer is illustrated. Second represents the ultrasonic beam reaching to particle/scatterer. Third shows the scattering in multiple direction of ultrasonic wave. The last one demonstrates the small amount of acoustic density returns or reflected back to the transducer.

3.3. Particle Size Determination with Attenuation Coefficient

The coefficient of ultrasonic attenuation and ultrasonic backscattering in suspensions depend on the particle size distribution of the particles and the concentration of particles in the suspension (Volker & de Kroon, 1998).

Vibration and oscillation occur when a particle presented an ultrasonic wave, and this causes secondary ultrasonic waves that are formed by the particle. So, occurrence of waves that are send to various directions related to ultrasonic waves, may cause a rise in the attenuation coefficient. In most suspensions, one or two above mechanisms often dominates overall attenuation in a frequency region. Visco-inertial and thermal loss mechanisms usually dominate at relatively low frequencies, on the other hand, at higher frequencies internal absorption and scattering losses are usually dominant (McClements, 1996). Attenuation arises by absorption which is the alteration in microstructure and physical properties. Shape and macroscopic structure of the media lead to attenuation that is formed by diffraction and scattering (Pandey, 2019). When, ultrasonic waves emit into an environment and dispersed as they encounter with the inhomogeneous part, part of the ultrasonic waves scatter. This non-homogeneity represents any difference in density or bulk modulus within the system. Relation between the wavelength of the ultrasonic wave and the size of inhomogeneity represented in the media leads to this phenomenon (Karakaş, 2016; Støylen, 2009). Ultrasonic wavelength and the particle size relation is the key point factor for the scattering mechanism. If the wavelength is much higher than the particle size, scattering of the propagating wave occurs in all directions. However, if the wavelength is much lower than the particle size or same size, half of the sound waves are gathered

behind the particle to create a sharp-edged shadow, and the other half is scattered. Attenuation is dependent on the scattering when particle size is in the same order of the wavelength (Karakaş, 2016; Morse & Ingard, 2014). Therefore, in this study scattering phenomenon is dominant due to high frequency and the absorption is neglected because it is assumed to be no occurrence of changes in the physical environment.

Additionally, Ultrasonic method benefits from frequency dependent ultrasonic velocity or attenuation coefficient of dispersion measurements to procure concentration and the size distribution of the particles in the suspension (McClements, 1996). In ultrasonic methods, concentration is obtained by the attenuation coefficient and the attenuation coefficient proportional to the concentration of a suspension. As particles presence in a suspension increases, concentration of the suspension increases, attenuation increases. More particles mean more scattering formation that leads to attenuation increase (Alba, Crawley, Fatkin, Higgs, & Kippax, 1999).

CHAPTER 4

EXPERIMENTAL METHODS

4.1. Void Fraction and Density Calculation of Sand

Sand particles are obtained from a quarry in Ankara. For particle size determination a Sieve analysis is performed. 38 μm, 63 μm, 75 μm, 90 μm, 150 μm meshed Retsch Test sieves are used for sieving. Retsch Sieve Shaker is operated for 20 minutes for amplitude of 80. Different particle size weights are given in the tables below. For first sieve analysis 38 μm, 63 μm, 90 μm, 150 μm sized test sieves are used. These different percentage of masses are mixed and total of 101.64 gram of sand is obtained for the first sieve analysis. The first sieve analysis and the percentage of sand mixture is given in Table 2. Same procedure is applied for smaller particle size of Test sieves for second sieve analysis. This time 38 μm, 63 μm, 75 μm, 90 μm sized sieves are used. Also, particles from first sieve analysis is used for second sieve analysis in order to increase total sand mass. Total of 223.82 gram of sand is obtained for the second sieve analysis and the sand mixture data is given in the Table 3.

Figure 13: Retsch Test Sieve

Figure 14: Retsch Sieve Shaker

Table 2: Sieve Analysis 1

Particle Size d_p (μm)	Mass (g)
$38 < d_p < 63$	4.69
$63 < d_p < 90$	28.01
$90 < d_p < 150$	68.94
Total	101.64

Table 3: Sieve Analysis 2

Particle Size d_p (μm)	Mass (g)
38< d_p< 63	34.44
63< d_p< 75	70.47
75< d_p< 90	118.91
Total	223.82

4.2. Void Fraction and Density Calculation of Sand

For the porosity calculation, a 100 ml container was filled with sand particles. First the weight of the empty container and then the sand filled container was measured and sand weight was determined. Then container that is filled with sand is taken and distilled water is poured until all the sand is wetted. From the volume of added distilled water, void fraction the sand is obtained. Sand mass and volume of the sand is used to calculate sand density. Sand absorption of water is assumed to be negligible. This procedure was repeated three times and the average of the three measurement are taken as sand density. Void fraction for three different measurements is given in Table 4. Also, sand masses, volumes and the average density are given in Table 5.

Table 4: Void Fraction of sand particles

Sand Volume (ml)	Distilled Water Volume (ml)	Void Fraction (φ)
100	35	0.35
100	33	0.33
100	36	0.36

Table 5: Density Calculation of sand particles

Sand Mass (g)	Sand Volume (ml)	Density(kg/m^3)
177.71	65	2734
173.80	67	2674
177.89	64	2779
Average Density		2729

4.3. UDV DOP 2000

Ultrasonic Doppler Velocimeter is used for fluid velocity measurements in a medium. However, in this study with the proper handling it is used for concentration determination not for the velocity. Experimental procedure is performed firstly by arranging the data of DOP 2000. Primarily, DOP 2000 program is initiated, and the appropriate variables are set. For 1 MHz probe, emitting frequency is set as 1 MHz and emitting power is chosen as Low. Also, Emit and Receive on the same transducer option is chosen in any experiment to be done. Resolution of the system is chosen as 2.44 mm for 3250 ns. Then, Pulse Repetition Frequency (PRF) is automatically taken as 7812 Hz. Time Gain Control (TGC) is set to Uniform and Value is fixed to 6 dB in order to obtain the full data in every measurement.

Figure 15: UDV DOP 2000

Figure 16: Ultrasonic Probe

4.4. Experimental Procedure

Experimental setup contains a 10 cm × 10 cm × 50 cm rectangular prism open top container made of plexiglass. All the measurements were taken from this container. Also, UDV DOP 2000 and ultrasonic probes are used. Ultrasonic gel is used for enhancing the contact surface of ultrasonic probe and the Plexiglass container. Sand suspension are prepared by measuring relevant sand weights and they are completed to 2500 ml by distilled water.

Figure 17: Plexiglass container

4.4.1. Calibration of Sand Suspension

Firstly, in order to reach attenuation of sand suspension a reference is needed. Since, sand suspensions are prepared with distilled water, distilled water measurements are made with plexiglass container, ultrasonic probe and the DOP 2000 device. Amplitude values of distilled water are recorded several times. Then, average value is taken for the distilled water.

After obtaining distilled water data, sand suspension calibration is performed. In order to reach sand calibration data for different weight percentages six different

concentration values are chosen. 1%, 0.75%, 0.5% 0.25% 0.125% and 0.0625% weight percent suspensions are prepared with weighing proper amount of sand which are given in the Table 6. Then they put in a volumetric flask and each time they are filled with distilled water up to 1 Liters.

Table 6: Data of calibration suspensions

Sand Weight (gr)	Weight Percentage (%)
0.625	0.0625
1.25	0.125
2.5	0.25
5	0.50
7.5	0.75
10	1

After carrying out the calibration experiment, 1 MHz probe is fixed to the UDV device, then ultrasonic gel is spread on to the probe tip. After that ultrasonic probe is leaned towards the container filled with sand suspension of %1 weight percent. This time, in order to create a set up like an Andreasen Pipette environment for 20 cm solution, a 1% weight percent suspension is prepared with 25 grams of sand particles and it is completed to 2500 ml by adding distilled water. For 2% sand suspension 50 grams of sand particles are completed to 2500 ml by distilled water. Ultrasonic probe was fixed at five centimeters above the bottom of the plexiglass container with the help of a clamp and the suspension is added until its level becomes 25 cm from the bottom. Hence a distance of 20 cm between suspension surface and probe is achieved. Ultrasound probe level corresponds to the concentration measurement location. As soon as sand suspensions are prepared and poured into the plexiglass container, experiments are initiated. For predetermined time intervals ultrasound amplitude data are taken by the Ultrasonic Instrument. Data are recorded each chosen time.

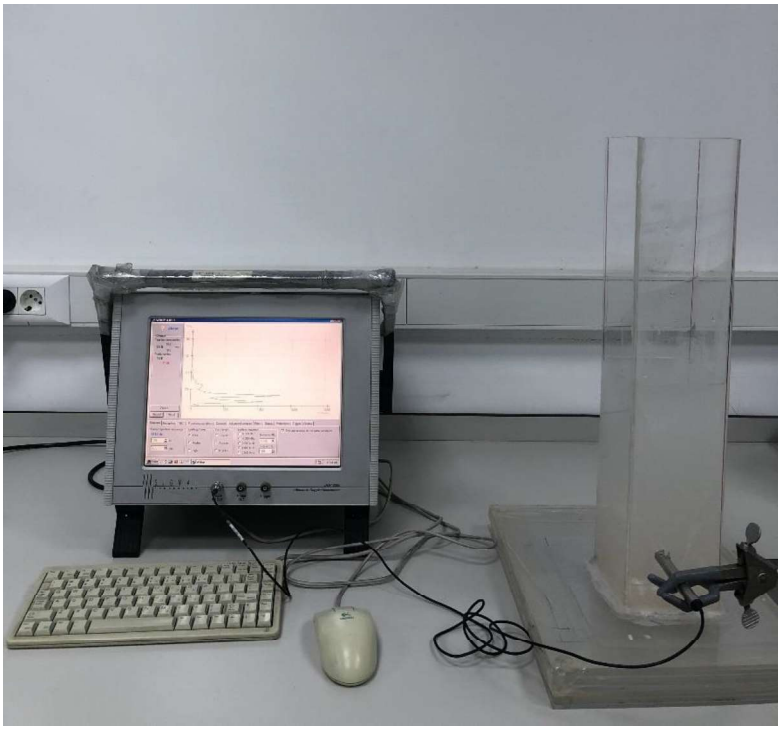

Figure 18: Experimental Setup

Same procedure is applied for second set of experiments, but for 2% weight percent suspension another calibration is performed. For 2% weight percent suspensions, different sand weights and 2500 ml distilled water is used. Different sand weights for second set experiments calibration data are given in the Table 7.

Table 7: Data of calibration suspensions of second set of experiments (2% sand suspension)

Sand Weight (gram)	Weight Percentage (%)
50	2.0
45	1.8
40	1.6
35	1.4
30	1.2
25	1.0
20	0.8
15	0.6
10	0.4
5	0.2
2.5	0.1

CHAPTER 5

RESULTS AND DISCUSSION

In order to calculate values of attenuation, amplitudes of each concentration for calibration and distilled water are measured. Ultrasonic Instrument measurements are performed according to the set values in the table below. These values are chosen for 1 MHz frequency.

Table 8: Ultrasonic Instrument Set Values

Frequency (MHz)	1
Emitting Power	Low
PRF (Hz)	7812
Resolution (mm)	2.44
TGC (dB)	6

With the Equation 31, attenuation coefficient is calculated. (Buckingham & Richardson, 2002) Attenuation coefficent is calculated in the unit of dB/m from the Equation 33.

$$\alpha = \frac{1}{2d} ln \left(\frac{A_w}{A_p}\right) \tag{33}$$

For the first set of experiments, maximum peak in the distilled water environment is around 1390 mV. For preventing any errors during the measurements, for distilled water, measurements repeated three times, and the average value of the amplitude was 1387.5 mV at 1 MHz.

Table 9: Different concentrated suspension Amplitude readings

Weight Percent (%)	Amplitude
0.0625	1368.9
0.125	1346.8
0.25	1315.3
0.50	1272.3
0.75	1230.1
1	1210.1

Table 9 shows that as concentration of a suspension increases, amplitude readings decrease. This can be explained by the fact that with increasing particle concentration, sound waves travel hardly. Particle amount increase affects the sound waves progression through the medium and as the concentration increases scattering increases and therefore amplitude values are decreasing.

After these measurements of different concentrated suspensions, attenuation coefficient of each six different concentrations are calculated according to Equation 33.

Table 10: Calibration data with attenuation coefficient

Weight Percent (%)	Attenuation Coefficient (dB/m)
0.0625	0.067
0.125	0.148
0.25	0.267
0.50	0.433
0.75	0.602
1	0.684

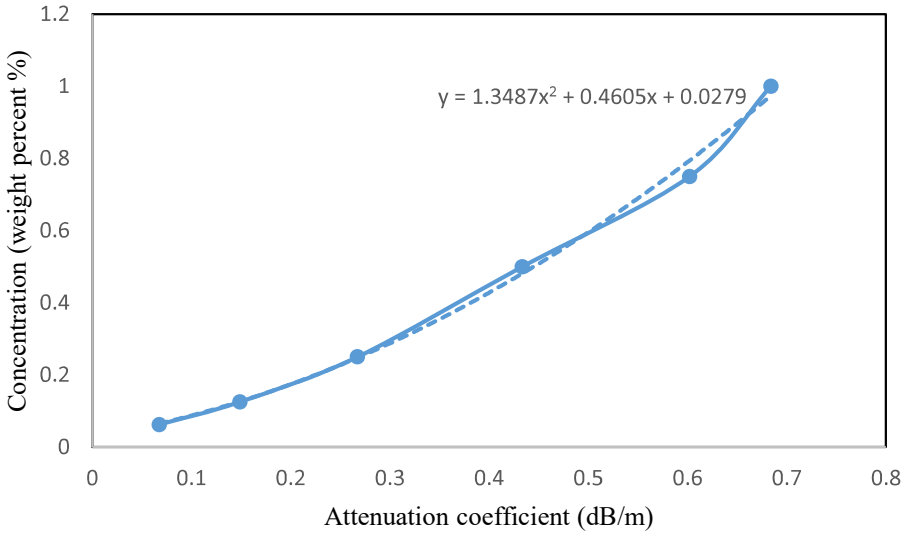

Figure 19: Calibration graph of sand suspensions at different concentration versus attenuation coefficient

From the Figure 16 attenuation coefficient to concentration calibration from attenuation equation is obtained that is the Equation 34.

$$y = 1.3487x^2 + 0.4605x + 0.0279 \quad (34)$$

Before beginning the settling experiments. Some calculations must be done to obtain the times of the measurements with UDV using Equation 30.

In Equation 30, μ is dynamic viscosity of water at 20℃, h is the settling height, and, in the setup, it is adjusted as 20 cm. $(\rho_p - \rho_f)$ is the density difference between sand particles and water. g is the gravitational acceleration. For example, when d is taken as for the smallest particle 38 μm and the largest particle 150 μm time of settling is calculated as 2.5 minutes and 10 seconds respectively. Moreover, for the second set of experiments these settling times are calculated for the smallest particle 38 μm and the largest particle 90 μm as 2.5 minutes and 26 seconds respectively.

After obtaining calibration graph and a polynomial fit for the calibration graph, for two sets of experiments; settling experiments are started. And the first set of the settling experiment is performed, amplitude versus time graph is given below. In the

Figure 17 there is a maximum for Amplitude data, after the maximum occurs in the Figure Amplitude remains constant afterwards. Amplitude reached its maximum value around ten minutes then it fluctuated in small proportions.

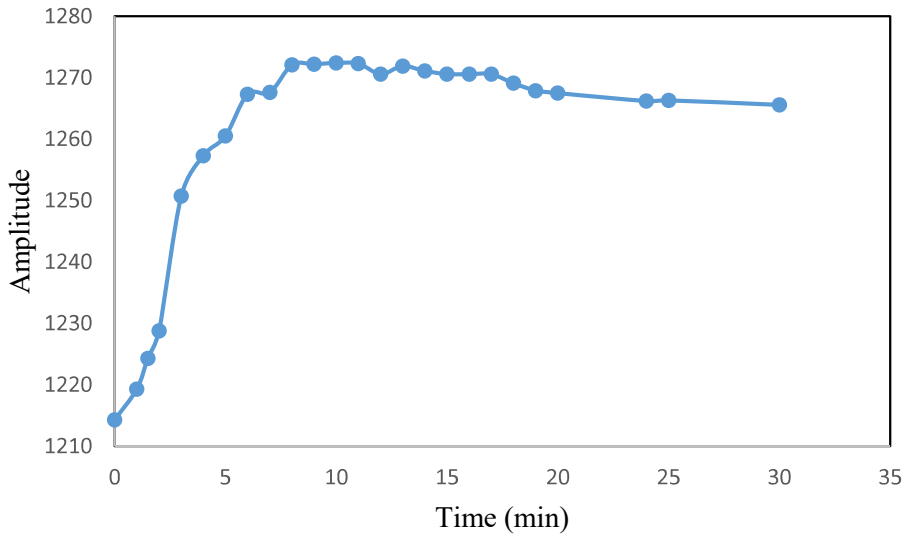

Figure 20: Amplitude versus time of the settling of 1% weight percent sand suspension

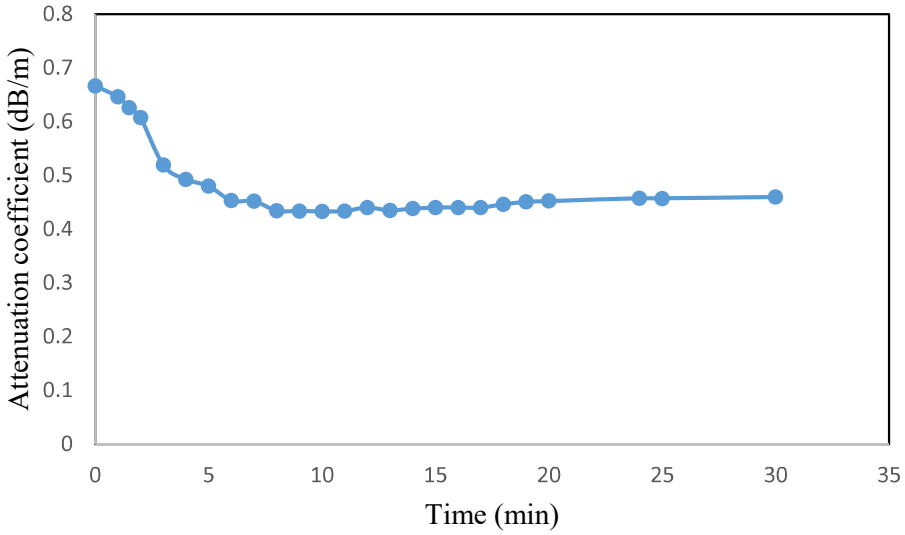

Figure 21: Attenuation coefficient versus time of the settling experiment of 1% weight percent sand suspension

The amplitude versus time raw data is converted to attenuation coefficient versus time as shown in the Figure 18, with the help of calibration graph and Equation 33, attenuation versus time plot is expressed as the concentration versus time graph that is given in the Figure 19.

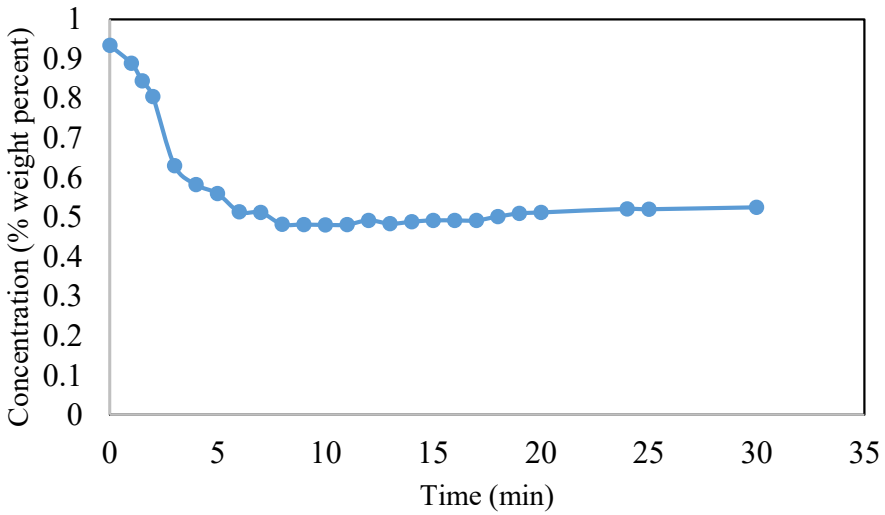

Figure 22: Concentration versus time of the settling experiment of 1% weight percent sand suspension

According the calculations, largest particle will be settled in ten seconds and the smallest particle will settle in two and a half minutes. In the experiments, it is seen that all the settling phenomena appears within first ten minutes. Then, the concentration of the suspension remains essentially unchanged. Therefore, concentration data until ten minutes are taken for the particle size analysis. Particle size of the settling suspension for each time interval is calculated from Equation 30 which is known as Andreasen Equation (Saklara et al., 2000; Ulusoy et al., 2007).

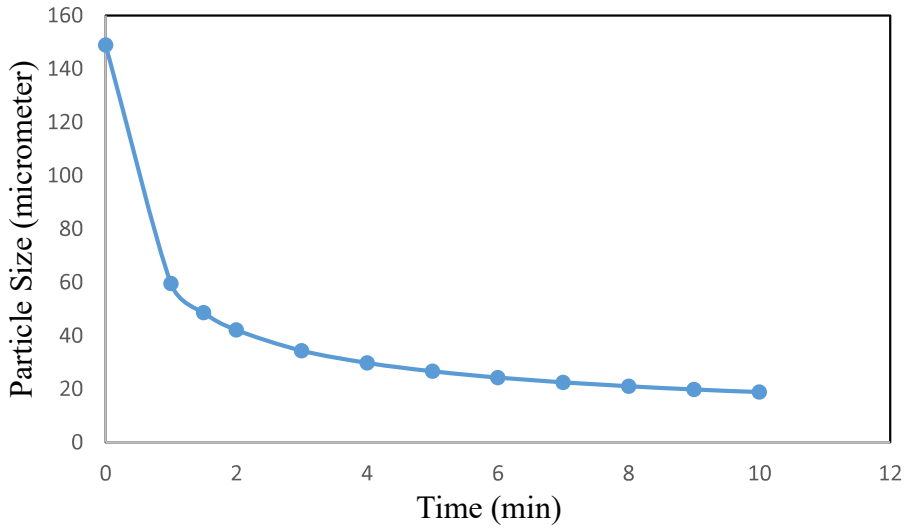

Figure 23: Particle Size versus Time calculated according to Andreasen Equation

In the Figure 21, obtaining the data from Figure 20, attenuation coefficient versus time concentration versus time of three experiments is extracted by using the calibration data and the formula. Much alike in the attenuation coefficient versus time graph, concentration versus time graph shows that data of Set 2 oscillated above the data of Set 1 and data of Set 3 is oscillated below the Set 1 data after ten minutes are finished. This can be tied to the physical conditions. Such as different particles are used for each set of experiments and since they are taken from the sand mixture; sizes they can be taken as in different ratios of different sizes. Also, each experiment is performed at

different times, and this might lead to various environmental conditions. For example, sound waves are affected by even experimental setup is exposed to vibrations. Impact on to the experiment bench can create undesired vibrations. Moreover, even the devices used in neighboring laboratories might cause vibrations and might affected irregularities in amplitude readings.

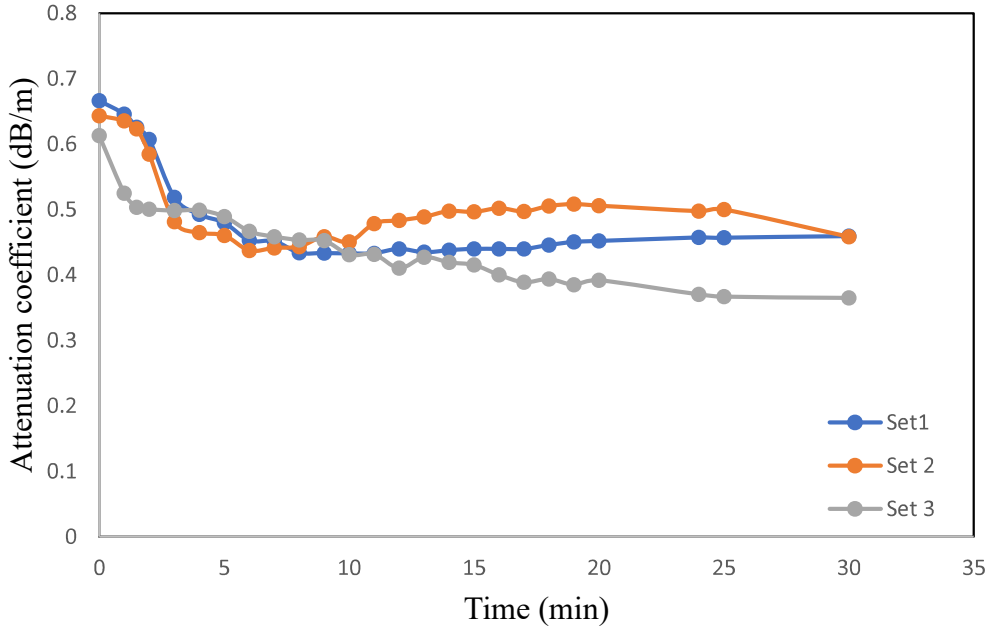

Figure 24: Attenuation coefficient comparison of three settling experiments

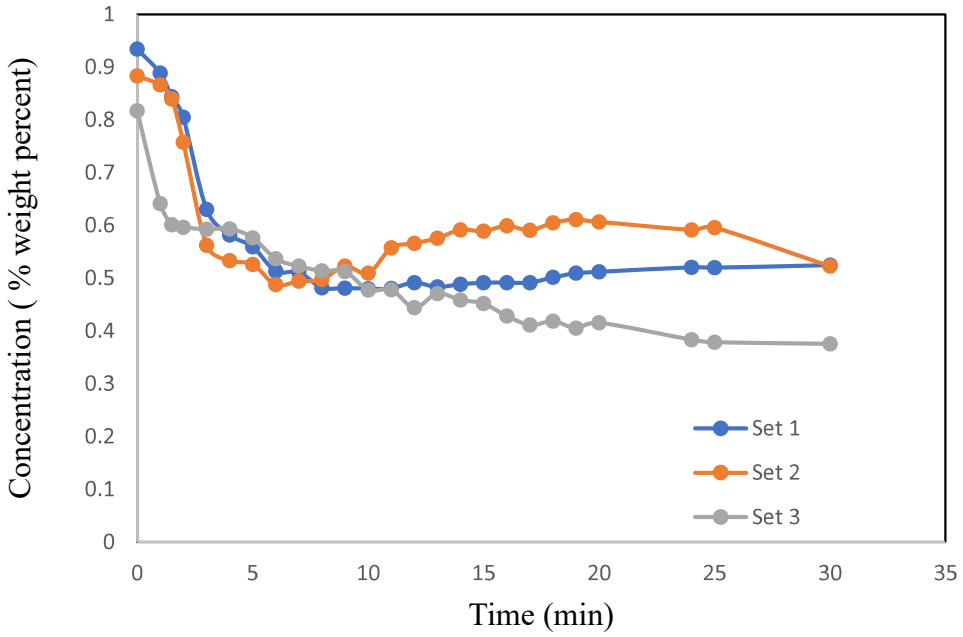

Figure 25: Comparison of concentration values of three different settling experiments

Furthermore, three separate experiments of 1% sand suspensions are done in order to show the reproducibility of the experiments. In the Figure 22 all three sets of experiments, are shown in the graph. The graph shows attenuation versus time. Attenuation of the ultrasonic waves are decreasing by time as expected due to settling of larger particles and then the smaller particles. Due to lower particle size, scattering of the sound waves gets weaker because larger the particle size larger the scattering and the more the attenuation of the sound waves. Additionally, all the three experiments have shown similar results. However, in Set 2 after ten minutes period, attenuation results are shown the fluctuation in the above of Set 1 and in the Set 3 attenuation results fluctuated below the results of Set 1. This can be explained by the physical conditions explained above. Also, all three experiments different suspensions are prepared and the different particle sizes in the sand mixture can cause the diversity in the attenuation results.

After the particle sizes are calculated, concentration difference of each time interval versus particle size differences of the data is given in the Figure 23.

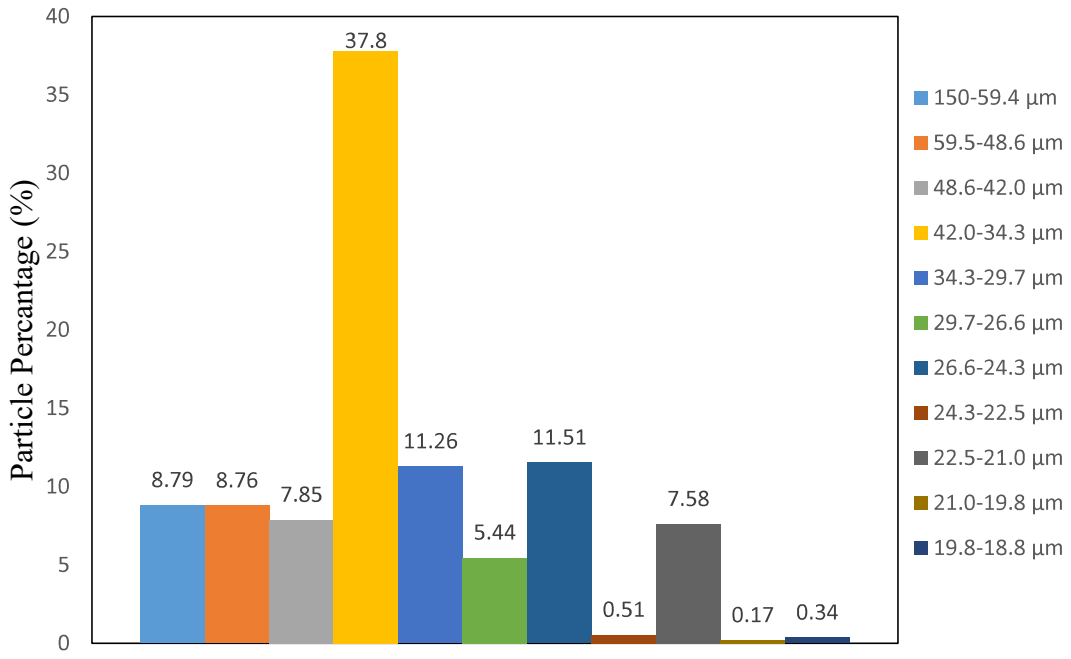

Figure 26: Particle Size versus Concentration

Moreover, what ratio of particle sizes the suspension have is given in the Table 11.

Table 11: Particle size range, concentration and percentage of each particle size range

Particle Size (μm)	Concentration (%)	Particle Size Percent in the Suspension
150 – 59.54	0.030	8.79
59.54 – 48.61	0.029	8.76
48.61 – 42.09	0.026	7.85
42.09 – 34.37	0.126	37.80
34.37 – 29.76	0.037	11.26
29.76 – 26.62	0.018	5.44
26.62 – 24.30	0.038	11.51
24.30 – 22.50	0.002	0.51
22.50 – 21.04	0.025	7.58
21.04 – 19.84	0.001	0.17
19.84 – 18.82	0.001	0.34

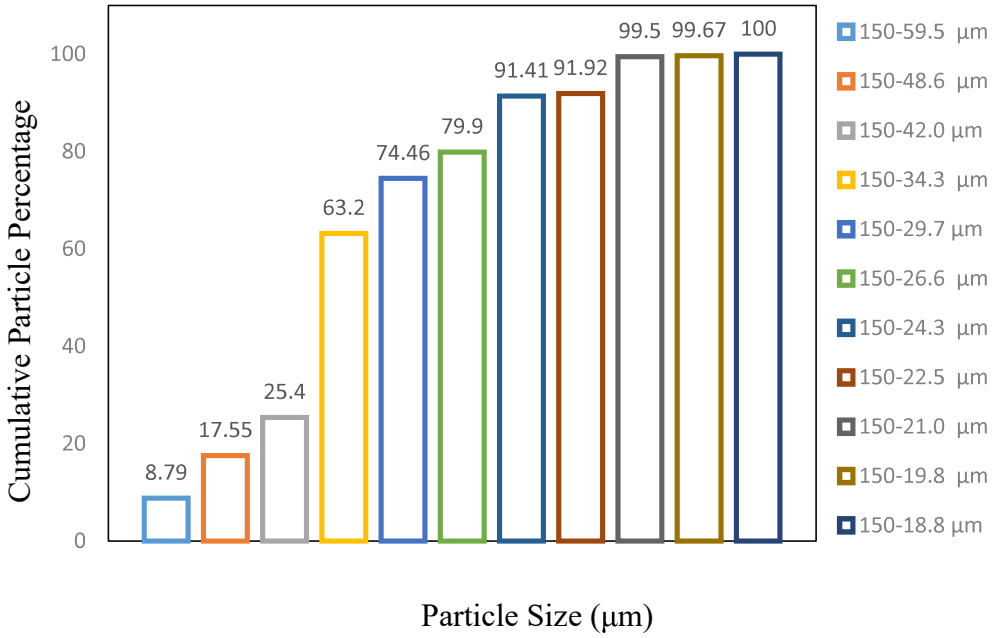

Figure 27: Particle Size versus Particle Percentage

Figure 27 represents the experimental results of the cumulative particle size distribution of 1% sand suspension.

Furthermore, from the sieve analysis general particle size is obtained and it is shown in the Table 12. It presents that total of 101.64 grams of sand contains 4.61% of particles of 38 μm between 63 μm, 27.56 % of 63 μm to 90 μm and finally, 67.83% of particles are between 90 μm to 150 μm.

Table 12: Weight Percent of particle size ranges from first sieve analysis

Particle Size (μm)	Mass (g)	Weight Percent (%)
38-63	4.690	4.610
63-90	28.01	27.56
90-150	68.94	67.83
Total	101.64	100

In the Table 13, data of particle from theoretical information and the combination of the experimental data from the settling experiments, concentration difference and the particle sizes are given.

Table 13: Particle size range, concentration and percentage of each particle size range

Particle Size (μm)	Concentration (%)	Particle Size Percent in the Suspension
150 – 59.54	0.030	8.79
59.54 – 48.61	0.029	8.76
48.61 – 42.09	0.026	7.85
42.09 – 34.37	0.126	37.80
34.37 – 29.76	0.037	11.26
29.76 – 26.62	0.018	5.44
26.62 – 24.30	0.038	11.51
24.30 – 22.50	0.002	0.51
22.50 – 21.04	0.025	7.58
21.04 – 19.84	0.001	0.17
19.84 – 18.82	0.001	0.34

If the sieve analysis and the Table 13 are compared, it is shown that sieve analysis is given a particle size range in restricted particle sizes due to sieves are produced standard sizes. Then, the settling experiment results shows that, the suspension contains 8.8% of particles in the range of 150 μm to 59.5 μm. 16.6% of the suspension contains the particles in the size of 59.5 μm to 42 μm. 66% of the suspension contains particle sizes between 42 μm to 24.3 μm. 8.6% of the suspension represents the particles smaller than the 24.3 μm. Settling experiments shows that majority of the suspension contains particle size between 42 μm to 24.3 μm that is 66% percent. However according to sieve analysis there should be no particles smaller than the 38 μm. As a matter of fact, from settling experiments 8.6% of particle mixture has a particle size smaller than 24.3 μm. This discrepancy may occur due to many reasons. First, it can be explained by during the sieve analysis particles smaller than 38 μm may not pass through the sieve. Second, experimental data and the theoretical data

usually not give the same outcomes. Finally, the experimental setup can be affected by the user and physical conditions that cannot be regulated.

Primarily, for the second set of experiments, calibration for 2% sand suspension is carried out. Calibration data for second set of experiments are given in the Table 14.

Table 14: Different concentrated suspension Amplitude readings

Weight Percent (%)	Amplitude
2	1229.9
1.8	1290.4
1.6	1306.3
1.4	1326.0
1.2	1356.3
1	1363.9
0.8	1385.4
0.6	1394.6
0.4	1404.8
0.2	1435.4
0.1	1454.0

Table 15: Calibration data with attenuation coefficient

Weight Percent (%)	Attenuation (dB/m)
2	0.897
1.8	0.656
1.6	0.595
1.4	0.520
1.2	0.407
1	0.380
0.8	0.301
0.6	0.268
0.4	0.232
0.2	0.124
0.1	0.060

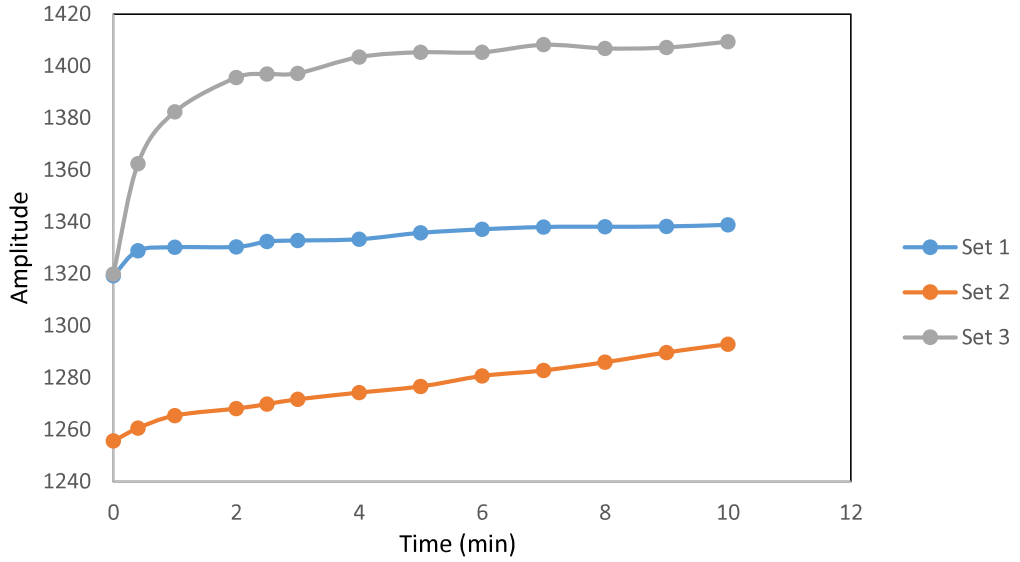

Figure 28: Amplitude versus time of the settling of 2% weight percent sand suspension for three different sets of experiments

Amplitude readings for 2% weight percent sand suspension for three different sets of experiments are given in the Figure 25. After obtaining Amplitude versus time graph, it is converted to attenuation versus time graph with the Equation 33.

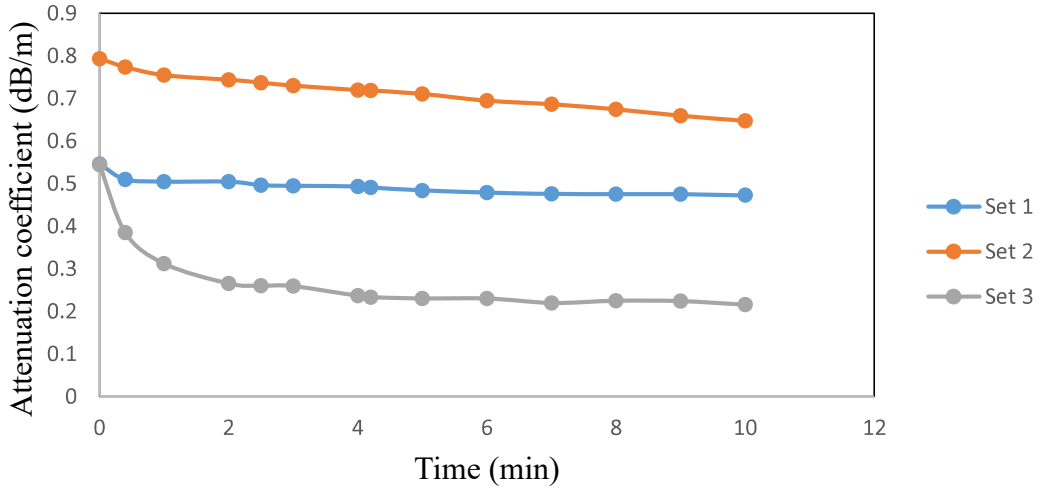

Figure 29: Attenuation coefficient versus time of 2% sand suspension for three different set of experiments

In the Figure 26, attenuation coefficient versus time graph is given for 2% concentrated sand suspensions for three different sets of experiments. Attenuation coefficients of three experiments show that as time passes, attenuation of the suspension is reduced. This reduction can be explained by the larger particles settle first and the smaller particles settle latter that leads to ultrasound waves are attenuated less as time goes by due to smaller particles affect slightly ultrasound waves.

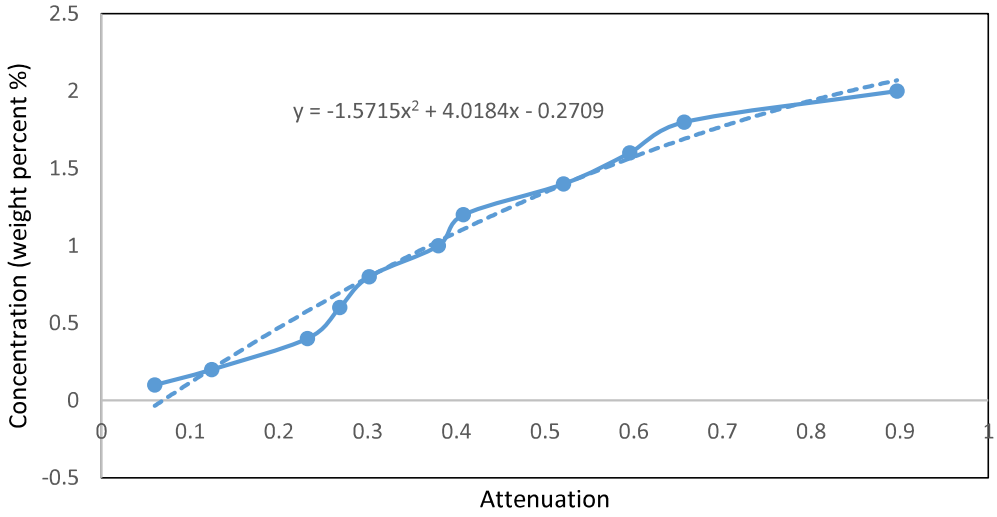

Figure 30: Calibration graph of sand suspensions at different concentration versus attenuation (for second set of experiments)

Calibration equation for attenuation coefficient conversion to concentration for second set of experiments is given by the Equation 35.

$$y = -1.5715x^2 + 4.0184x - 0.2709 \quad (35)$$

In the Figure 27, obtaining the data from Figure 26, using data from attenuation coefficient versus time graph and with the help of second calibration information, concentration versus time of three different experiments are shown. Like the attenuation coefficient versus time graph, concentration versus time graph shows that data of Set 2 and Set 1 is close to each other. However, set 3 is reached a higher concentration decrease in the 10 minutes of experiments.

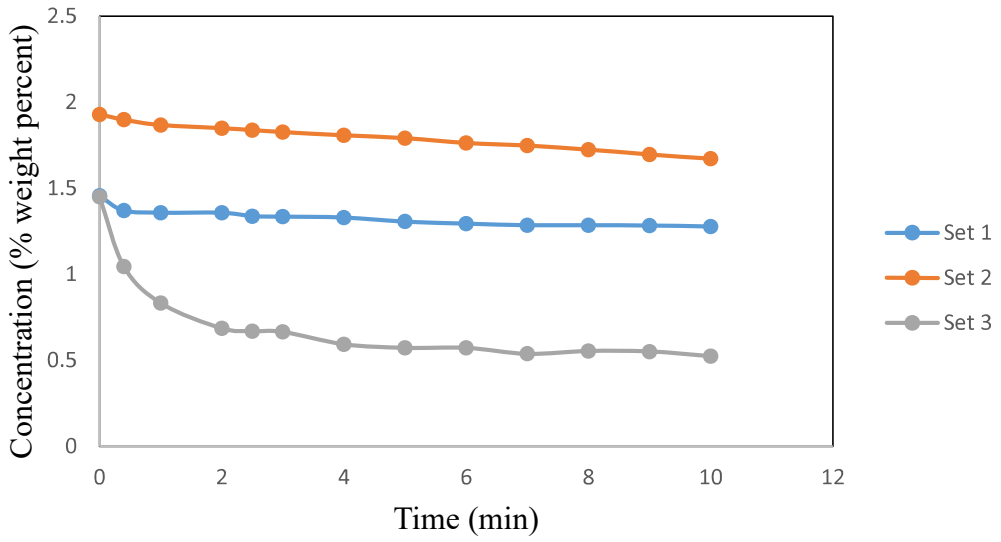

Figure 31: Concentration versus time of 2% sand suspension

According the calculations, largest particle will settle in 26 seconds and the smallest particle will settle in two and a half minutes. In the experiments, it is seen that mostly the settling phenomena appears in the first four minutes. Then, the concentration of the suspension decreases slowly respectively to beginning of the settling. Therefore, concentration data until five minutes are taken for the particle size analysis. Particle size of the settling suspension for each time interval is calculated from Andreasen Equation (Saklara et al., 2000; Ulusoy et al., 2007).

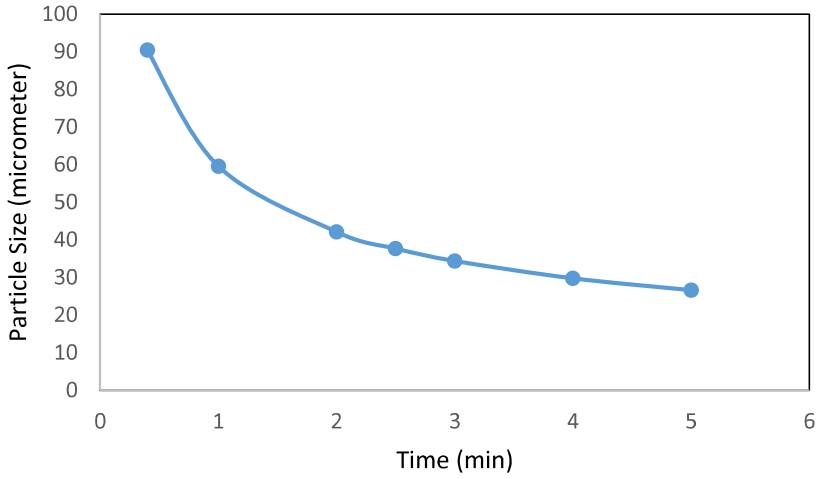

Figure 32: Particle Size versus Time calculated according to Andreasen Equation

From settling experiments for second sieve analysis, particle size ranges, concentration of each range and percentage of particle sizes for each range that are obtained from experimental results, is given in the Table 16.

Table 16: Particle size range, concentration and percentage of each particle size range

Particle Size (μm)	Concentration (%)	Particle Size Percent in the Suspension
90.44-59.54	0.406	46.2
59.54-42.09	0.213	24.2
42.09-37.65	0.147	16.6
37.65-34.37	0.016	1.82
34.37-29.77	0.003	0.39
29.77-26.63	0.073	8.28
26.63-24.30	0.021	2.39

In order to compare experimental results above with the sieve analysis general particle size is obtained and it is shown in the Table 17. It presents that total of 223.82 grams of sand contains 15.38 % of particles of 38 μm between 63 μm, 31.49 % of 63 μm to 90 μm and finally, 53.13 % of particles are between 90 μm to 150 μm.

Table 17: Weight Percent of particle size ranges from second sieve analysis

Particle Size d_p (μm)	Mass (g)	Weight Percent (%)
38< d_p< 63	34.44	15.38
63< d_p< 75	70.47	31.49
75< d_p< 90	118.91	53.13
Total	223.82	100

In the purpose of comparison between the sieve analysis and the experimental data Tables 16 and 17 are used. Sieve analysis is given a limited particle size range due to standard production of sieves. Other issue, that is the settling experiment data indicates that, the suspension contains 46.2% of particles in the range of 90 μm to 59.5 μm. 24.2% of the suspension contains the particles in the size of 59.5 μm to 42 μm. 16.6% of the suspension contains particle sizes between 42 μm to 37.6 μm. 12.9% of the suspension represents the particles smaller than the 37.6 μm. Settling experiments shows that majority of the suspension contains particle size between 90 μm to 59.5 μm that is 46.2% percent. On the other hand, sieve analysis also contains majority of the concentration percentage between 90 μm and 75 μm. Although, the sieve analysis and the settling experiment data do not fit exactly, they otherwise agree with each other. According to sieve analysis there should be no particles smaller than the 38 μm however, from settling experiments 12.9% of particle mixture has a particle size smaller than 37.6 μm. This divergence in the results can occur due to physical reasons. For example, particles smaller than 38 μm may not pass through the sieve. Second, experimental data and the theoretical data usually not give the same outcomes. The experimental setup can be affected by the user and physical conditions that cannot be regulated.

On the condition that calibration equations for both sets of experiments are compared, Equation 34 has positive tendency for concentration conversion, on the other hand, Equation 35 has negative tendency for concentration conversion. The reason for this

can be the data frequency that are taken for the calibration experiments. More data were taken for second set of experiments and this led to difficult fit of equation in the second calibration graph and therefore equation resulted in negative tendency. Furthermore, if the results from second set of experiments that is carried out with particle size range of 38 μm to 90 μm and the first set of experiments that is carried out with particle size range of 38 μm to 150 μm, are compared it can be deduced that second set of experiments achieved better results. Smaller particle size range can be considered as the reason for the better results due to Stokes' Equation application range. Besides that, Ultrasonic Instrument gives more sensitive and accurate results for the smaller particle sizes. Ultrasonic device produced more fluctuating data for larger particle sizes and the more noise is observed for the larger particle size conditions. However, for the first set of experiments that is larger particle size range has more reproducible results than the second set of experiments that is smaller particle size range. Reproducibility of second set of experiments is worse due to drawbacks attained from the experimental setup. Experimental setup is not too rigid, and it affects the readings of amplitudes every time differently.

.

CHAPTER 6

CONCLUSIONS

Based on theoretical and the experimental results that are obtained in this study, the following conclusions can be drawn.

The sieve analysis is made for two sets of experiments. For first set of experiments mixture of sand particles between 38 μm to 150 μm is prepared. For the second set of experiments, 38 μm to 90 μm were the upper and lower limit of particle size range.

The amplitude of the readings from Ultrasonic Instrument shows that, as concentration increases amplitude data are decreasing. Water has a higher amplitude value than the suspension amplitudes. It is clearly shown in the calibration experiments. On the other hand, as the amplitudes are decreasing by the increasing concentration of suspensions, the opposite is valid for the attenuation coefficient values.

Settling of particles are used in this study for particle size determination. The Andreasen equation is used for the particle size calculations from times of settling experiment. Despite the calculations, mostly the settling phenomena takes places in the first ten minutes and generally for the first 5 minutes most of the concentration decrease occurs. However, calculations show that smallest particle will settle in the 2.5 minutes. Theoretical and the experimental data do not always match exactly with each other, but they do not show total opposite results. Even the results from both aspects can be considered very close to each other.

Settling experiment is used primarily for obtaining amplitudes of each time data than they are converted to attenuation data and attenuation coefficient data is converted to concentration values of each time. Concentration difference is calculated between each time and the particles sizes are calculated from the Andreasen equation; these culminates the particle size versus concentration data of the suspension.

According to sieve analysis, particle mixture contains 4.61% of particle size between 38 μm to 63 μm, 27.56% of particle size between 63 μm to 90 μm and 67.83% of particle size between 90 μm to 150 μm. The settling experiment results shows that, the 66% of the suspension contains particle sizes between 24.3 μm to 42 μm, 16.6% of the suspension contains the particles in the size of 42 μm to 59.5 μm and 8.8% of particles in the range of 59.5 μm to 150 μm. 8.6% of the suspension represents the particles smaller than the 24.3 μm. Settling experiments shows that majority of the suspension contains particle size between 42 μm to 24.3 μm that is 66% percent. 8.6% of particle mixture has a particle size smaller than 24.3 μm although sieve analysis shows that there should be no particles smaller than the 38 μm.

For second set of experiments, settling experiment data indicates that, the suspension contains 46.2% of particles in the range of 90 μm to 59.5 μm. 24.2% of the suspension contains the particles in the size of 59.5 μm to 42 μm. 16.6% of the suspension contains particle sizes between 42 μm to 37.6 μm. 12.9% of the suspension represents the particles smaller than the 37.6 μm. Settling experiments shows that generality of the suspension contains particle size between 90 μm to 59.5 μm that is 46.2% percent. On the other hand, sieve analysis also contains majority of the concentration percentage between 90 μm and 75 μm. According to sieve analysis there should be no particles smaller than the 38 μm however, from settling experiments 12.9% of particle mixture has a particle size smaller than 37.6 μm.

Furthermore, the inequality of the particle size and the particle size percentage from settling experiment and the theoretical calculations can be considered as wide. This can be explained by the user errors in physical conditions. Comparison of experimental and theoretical results show that this method cannot be used for obtaining particle size distribution. In order to get PSD for a suspension, the method used for obtaining particle size distribution in this thesis can be investigated in more detail. There should be more studies to be performed to fix the inconsistency between the experimental and the theoretical results of the particle size distribution. Also, with smaller particle sizes and particles with different densities and maybe in different

medium other than distilled water, experiments can be performed. This will lead to data diversity in every aspect of the experimental results.

REFERENCES

Alba, F., Crawley, G. M., Fatkin, J., Higgs, D. M. J., & Kippax, P. G. (1999). Acoustic spectroscopy as a technique for the particle sizing of high concentration colloids, emulsions and suspensions. *Colloids and Surfaces A: Physicochemical and Engineering Aspects*, *153*(1–3), 495–502. https://doi.org/10.1016/S0927-7757(98)00473-7

Allen, T. (2003). 7 - Gravitational sedimentation methods of particle size determination. *Powder Sampling and Particle Size Determination*, 359–391. https://doi.org/http://dx.doi.org/10.1016/B978-044451564-3/50009-7

Cheng, N.-S. (n.d.). *A Simplified Settling Velocity Formula For Sediment PArticle*. Singapore.

Concha, F. (2009). Settling velocities of particulate systems. *KONA Powder and Particle Journal*, *27*(27), 18–37. https://doi.org/10.1016/s0301-7516(99)00017-4

CPS. (2007). Introduction to Differential Sedimentation. *Analytical Ultracentrifugation*, *31*(0), 270–290. https://doi.org/10.1039/9781847552617-00270

Duran, P. K., Tekstil, E. Ü., Bölümü, M., Gör, A., Bahtiyari, M. I., Tekstil, E. Ü., Bölümü, M. (n.d.). *Ultrason teknolojisi*. (4), 155–158.

Hendee, W. R., & Ritenour, E. R. (2002). *Medical Imaging Physics, Ultrasound Waves*. Retrieved from https://www.k-space.org/ymk/Ultrasound_HO.pdf

Hijazi, A. (n.d.). *Introduction to Non-Destructive Testing Techniques Ultrasonic Testing*. 1–36.

Hwang, J. H. (n.d.). 1 - Principles of Ultrasound. In *Endosonography* (Fourth Edi). https://doi.org/10.1016/B978-0-323-54723-9.00001-4

Kahn, R. A., & Salgo, I. S. (2013). Principles and Physics: Principles of Ultrasound. *Perioperative Transesophageal Echocardiography: A Companion to Kaplan's Cardiac Anesthesia*, 14–17. https://doi.org/10.1016/B978-1-4557-0761-4.00002-5

Karakaş, Z. (2016). *Theoretical and Experimental Investigation Of Ultrasound Propagation In Packed Beds*.

Krishnamoorthy, S., Schmall, J. P., & Surti, S. (2016). PET physics and instrumentation. In *Basic Science of PET Imaging* (1st ed.). https://doi.org/10.1007/978-3-319-40070-9_8

McCabe, W. L., Smith, J. C., & Harriott, P. (n.d.). *Unit Operations of Chemical Engineering* (5th Editio). McGraw-HiII International Editons.

McClements, D. J. (1996). Ultrasonic Measurements Particle Size Analysis. *Encyclopedia of Analtyical Chemistry*, *54*(4), 1–8.

Modes of Sound Wave Propagation. (n.d.). Retrieved July 27, 2019, from https://www.nde-ed.org/EducationResources/CommunityCollege/Ultrasonics/Physics/modepropagation.htm

Morse, P. M., & Ingard, K. U. (2014). Theoretical Acoustic. *Igarss 2014*, (1), 1–5. https://doi.org/10.1007/s13398-014-0173-7.2

NDT Olympus. (2006). Ultrasonic transducers technical notes. *Technical Brochure: Olympus NDT, Waltham, MA*, 40–50. Retrieved from http://www.olympus-ims.com/pt/knowledge/%5Cnhttp://scholar.google.com/scholar?hl=en&btnG=Search&q=intitle:Ultrasonic+Transducers+Technical+Notes#1%5Cnhttp://scholar.google.com/scholar?hl=en&btnG=Search&q=intitle:Ultrasonic+transducers+technical+notes#1

Pandey, D. K. (2019). *We are IntechOpen , the world ' s leading publisher of Open Access books Built by scientists , for scientists*. https://doi.org/10.5772/10153

Povey, M. J. W. (2013). Ultrasound particle sizing: A review. *Particuology*, *11*(2), 135–147. https://doi.org/10.1016/j.partic.2012.05.010

Powles, A. E., Martin, D. J., Wells, I. T., & Goodwin, C. R. (2018). Physics of ultrasound. *Anaesthesia and Intensive Care Medicine*, *19*(4), 202–205. https://doi.org/10.1016/j.mpaic.2018.01.005

Saklara, S., Bayraktara, I., & Öner, M. (2000). İnce Tane Boyu Analizinde Kullanılan Yöntemler. *MADENCİLİK*, 29–47.

Støylen, A. (2009). Basic ultrasound , echocardiography and Doppler ultrasound Basic ultrasound , echocardiography and Doppler ultrasound. Retrieved December 1, 2019, from Ultrasound website: http://folk.ntnu.no/stoylen/strainrate/Basic_Doppler_ultrasound

Taylor, P. M. (2012). The physics of ultrasound. *Imaging and Technology in Urology: Principles and Clinical Applications*, *9781447124*, 23–26. https://doi.org/10.1007/978-1-4471-2422-1_6

Testino, A., Alberto, M., Cervellino, A., & Ludwig, C. (2015). Phase-resolved particle size distribution : New insight into material characterization. *Materials Letters*, *158*, 333–338. https://doi.org/10.1016/j.matlet.2015.06.051

Ulusoy, U., Yekeler, M., Biçer, C., & Gülsoy, Z. (2007). Combination of the particle size distributions of some industrial minerals measured by andreasen pipette and sieving techniques. *Particle and Particle Systems Characterization*, *23*(6), 448–456. https://doi.org/10.1002/ppsc.200500988

Wave Propagation. (n.d.). Retrieved July 27, 2019, from https://www.nde-ed.org/EducationResources/CommunityCollege/Ultrasonics/Physics/wavepropagation.htm

Weser, R., Wöckel, S., Hempel, U., Wessely, B., & Auge, J. (2013). Particle characterization in highly concentrated suspensions by ultrasound scattering method. *Sensors and Actuators A: Physical*, *202*, 30–36. https://doi.org/10.1016/J.SNA.2013.02.027

Zhiyao, S., Tingting, W., Fumin, X., & Ruijie, L. (2015). A simple formula for predicting settling velocity of sediment particles. *Water Science and Engineering*, *1*(1), 37–43. https://doi.org/10.1016/s1674-2370(15)30017-x

APPENDICES

A. Technical specifications DOP2000, model 2125

Emission

Emitting frequency	from 0.45 MHz to 10.5 MHz, step of 1 kHz
Emitting power	3 levels. Instantaneous maximum power for setting (approx.): low = 0.5 W, medium= 5 W, high= 35 W
Burst length	2, 4 or 8 cycles
Pulse repetition frequency	between 64 µs (48 mm) and 100'000 µs (7'875 mm), step of 1 µs

Reception

Number of gates	between3 and 1000, step of 1 gate
Position of the first channel	movable by step of 250 ns
Amplification (TGC)	Uniform, Slope, Custom Slope mode exponential amplification between two defined depth values. Value at both depths variable between -40dB and +40dB Custom mode User's defined values between -40dB and +40dB in cells. Variable number, size and position of the cells.
Sensitivity	> -100 dBm

Resolution

Sampling volume: lateral size defined by the acoustical characteristics of the transducer

Sampling volume: longitudinal size minimum value of 0.85 μs (0.64 mm) depends on spatial filter and burst lenght.
(approximate value, defined at 50% of the received)

Spatial filter from 50 KHz (3.9 mm) to 300 KHz (0.7 mm), step of 50 KHz

Display resolution: distance between the center of each sample volume selectable between 0.25 μs (0.187 mm) and 20 μs (15 mm), step of 0.25 μs.

Velocity resolution 1 LSB (maximum = 0.0091 mm/s; minimum = 91.5 mm/s) Doppler frequency given in a signed byte format

Ultrasonic processor

Doppler frequency computation based on a correlation algorithm

Wall filter stationary echoes removed by IIR high-pass filter 2nd order

Number of emissions per profile between 1024 and 8, any values

Detection level 5 levels of the received Doppler energy may disable the computation

Acquisition time per profile depends on PRF and number of emissions per profile minimum arround 2 to 3 ms

Filters on profiles moving average: based on 2 to 32000 profiles zero values included or rejected median, based on 3 to 32 profiles

Maximum velocity 11.72 m/s for bi-directional flow (at 0.5 MHz)

Velocity scale variable positive and negative velocity range.

Computation

Compute and display	velocity profile Doppler energy echo modulus velocity profile with echo modulus or Doppler energy velocity profile with velocity versus time of one selected gate velocity profile with flow rate versus time (circular section assumed) velocity profile with real time histogram echo modulus with real time histogram Doppler energy with real time histogram velocity profile with turbulence profile power spectrum of one selected gated 2D, 3D velocity filed (in option)
Statistics	mean, standard deviation, minimum, maximum
Velocity component	automatic computation of the projected velocity component
Replay mode	replays a recorded measure from the disk
Utility	freeze/run mode

Advanced features

measurement of the ultrasonic field acquisition of I and Q signals (8000 values can be recorded) emission and

	reception can be realized on separated connectors
Trigger	
Input	external signal (TTL) or keyboard action
Configuration parameters	high, low level, internal pull-up 4 KW
Delay	between 1 and 10’000 ms, step of 1ms
Acquisition procedure	selectable number of blocks of profiles
automatic record capability	
Memory/Files	
Internal memory	variable size, memorization from 2 to
32000 profiles	
Configuration parameters	10 saved configurations
Data file	Binary (include: ASCII short info blocks,
comments, all parameters, all data profiles)	
	ASCII(statistical information available)
Environment (may be changed)	
Operating system	Windows XP®
Processor	VIA Eden 800MHz
RAM	128 MBytes (up to 512 Mbytes in option)
Screen	12,4” TFT color, 800x600 VGA
Storage devices	Hard disk of 80 Gbytes
	CD-ROM Read/Write
Communication	2 serial ports
	1 parallel port (printer port)
	1 Ethernet 10 base T, RJ45
	1 external SGVA (simultaneous with TFT)
	2 PS2 port (mouse and keyboard)
	1 USB (Rev 1.10, type A)

US interface 50 ohm, BNC	Echo (max 0.7 Vp), output impedance of TTL high level pulse of 100 ns at each emission, BNC Logic level trigger input, pull up by 330 ohm. BNC US probe In/Out, BNC US emission connector BNC
Power supply	110 - 220 VAC, 50 - 60 Hz
Humidity	=< 80%
Temperature	5 - 35 degrees
Sizes	340x265x305 cm
Weight	13 Kg

Options

Multiplexer for 10 probes, internal or external

2D, 3D Ultrasonic Doppler Velocity measuring capability

Sound speed measuring unit

Notes

All values computed with a sound velocity of 1500 m/s (water), in the direction of the ultrasonic beam.

B. Error Margins for the Calibration Graphs

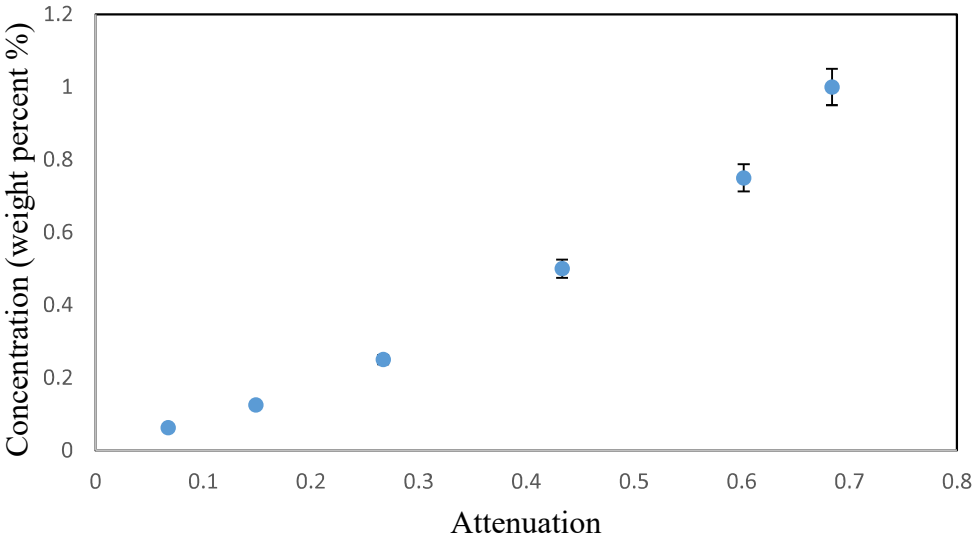

Figure 33: Error Margins for the first calibration graph

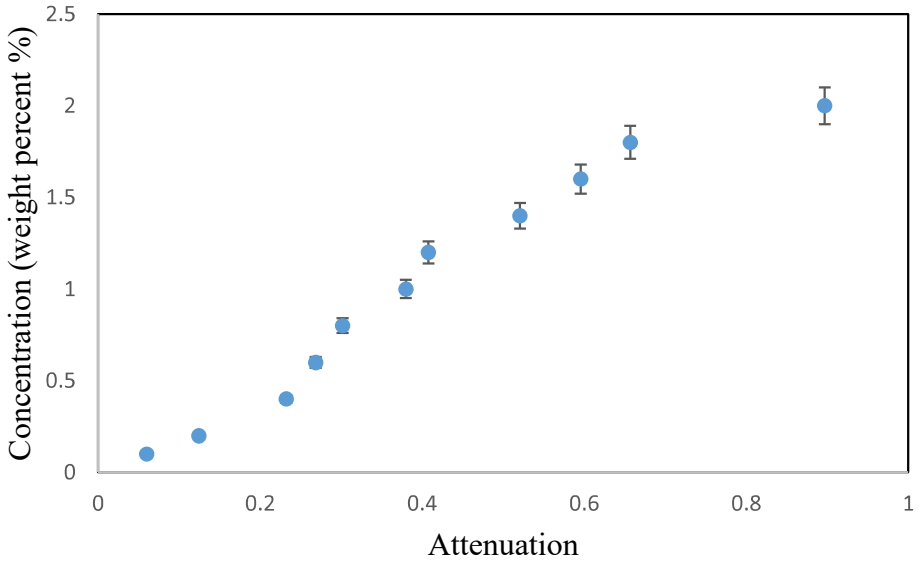

Figure 34: Error Margins for the second calibration graph